

1 **Radiocarbon dating of alpine ice cores with the dissolved organic carbon**  
2 **(DOC) fraction**

3

4 Ling Fang<sup>1,2,3</sup>, Theo M. Jenk<sup>1,3,\*</sup>, Thomas Singer<sup>1,2,3</sup>, Shugui Hou<sup>4,5</sup>, Margit Schwikowski<sup>1,2,3</sup>

5

6 \*Corresponding author: Theo M. Jenk (theo.jenk@psi.ch)

7 <sup>1</sup>Laboratory for Environmental Chemistry, Paul Scherrer Institute, CH-5232 Villigen PSI,  
8 Switzerland

9 <sup>2</sup>Department of Chemistry and Biochemistry, University of Bern, CH-3012 Bern, Switzerland

10 <sup>3</sup>Oeschger Centre for Climate Change Research, University of Bern, CH-3012 Bern,  
11 Switzerland

12 <sup>4</sup>School of Geographic and Oceanographic Sciences, Nanjing University, Nanjing, 210023,  
13 China

14 <sup>5</sup>School of Oceanography, Shanghai Jiao Tong University, Shanghai 200240, China

15	<b>Abstract</b>
16	

17 High-alpine glaciers are valuable archives of past climatic and environmental conditions. The  
18 interpretation of the preserved signal requires a precise chronology. Radiocarbon ( $^{14}\text{C}$ ) dating  
19 of the water-insoluble organic carbon (WIOC) fraction has become an important dating tool to  
20 constrain the age of ice cores from mid-latitude and low-latitude glaciers. However, in some  
21 cases this method is restricted by the low WIOC concentration in the ice. In this work, we  
22 report first  $^{14}\text{C}$  dating results using the dissolved organic carbon (DOC) fraction, which is  
23 present at concentrations of at least a factor of two higher than the WIOC fraction. We  
24 evaluated this new approach by comparison to the established WIO $^{14}\text{C}$  dating based on parallel  
25 ice core sample sections from four different Eurasian glaciers covering an age range of several  
26 hundred to around 20'000 years.  $^{14}\text{C}$  dating of the two fractions yielded comparable ages with  
27 WIO $^{14}\text{C}$  revealing a slight, barely significant, systematic offset towards older ages. ~~Our data~~  
28 ~~suggests comparable in magnitude with the analytical uncertainty. We attribute this to be~~  
29 ~~caused by offset to two effects of about equal size, but opposite in direction: (i) in-situ produced~~  
30  ~~$^{14}\text{C}$  contributing to the DOC resulting in a bias towards younger ages and (ii) incompletely~~  
31 ~~removed carbonate carbonates from particulate mineral dust ( $^{14}\text{C}$  depleted) contributing to the~~  
32 ~~WIOC fraction, with a bias towards older ages. The estimated amount of in-situ produced  $^{14}\text{C}$~~   
33 ~~in the DOC fraction is smaller than the analytical uncertainty for most samples. Nevertheless,~~  
34 ~~under extreme conditions, such as very high altitude and/or low snow accumulation rates,~~  
35 ~~DO $^{14}\text{C}$  dating results need to be interpreted cautiously. While in the during DOC extraction~~  
36 ~~procedure the removal of inorganic carbon is monitored to ensure complete removal, the for~~  
37 ~~completeness, the removal for WIOC samples was so far only assumed to be quantitative, at~~  
38 ~~least for ice samples containing average levels of mineral dust. Here we estimated an average~~  
39 ~~removal efficiency for WIOC samples was here estimated to be ~96%. We did not find any~~  
40 ~~indication of in-situ production systematically contributing to DO $^{14}\text{C}$  as suggested in a~~  
41 ~~previous of  $98 \pm 2\%$ , resulting in a small offset in the order of the current analytical uncertainty.~~  
42 ~~Future optimization of the removal procedure has the potential to improve the accuracy and~~  
43 ~~precision of WIO $^{14}\text{C}$  dating. With this study. By we demonstrate, that using the DOC instead~~  
44 ~~of the fraction for  $^{14}\text{C}$  dating is not only a valuable alternative to the use of WIOC fraction for~~  
45  ~~$^{14}\text{C}$  dating, the, but also benefits from a reduced required ice mass can be reduced to of~~  
46 ~~typically ~250 g, yielding a to achieve comparable precision of around  $\pm 200$  years or even~~  
47 ~~better if sample sizes typically required for WIO $^{14}\text{C}$  dating are used. This study shows approach~~  
48 ~~thus has~~ the potential of pushing radiocarbon dating of ice forward even to remote ~~and Polar~~  
49 ~~Regions, regions~~ where the carbon content in the ice is particularly low, ~~when applying the~~  
50 ~~DOC fraction for  $^{14}\text{C}$  dating.~~



## 52 **1 Introduction**

53

54 For a meaningful interpretation of the recorded paleoclimate signals in ice cores from glacier  
55 archives, an accurate chronology is essential. Annual layer counting, supported and tied to  
56 independent time markers such as the 1963 nuclear fallout horizon evident by a peak maximum  
57 in tritium or other radioisotopes, or distinct signals from known volcanic eruptions in the past  
58 is the fundamental and most accurate technique used for ice core dating. However, for ice cores  
59 from high-alpine glaciers this approach is limited to a few centuries only, because of the  
60 exceptional strong thinning of annual layers in the vicinity of the bedrock. Most of the current  
61 analytical techniques do not allow high enough sampling resolution for resolving seasonal  
62 fluctuations or detecting distinct single events in this depth range. Ice flow models, which are  
63 widely used to retrieve full depth age scales (e.g. Nye, 1963; Bolzan, 1985; Thompson et al.,  
64 2006), also fail in the deepest part of high-alpine glaciers due to the ~~complex bedrock~~  
65 ~~geometry-assumption of steady state conditions and the complexity of glacial flow and bedrock~~  
66 ~~geometry limiting realistic modeling of strain rates~~. Even with 3D models, which require  
67 extensive geometrical data, it is highly challenging to simulate a reasonable bottom age (e.g.  
68 Licciulli et al., 2020). This emphasizes the need for an absolute dating tool applicable to the  
69 oldest, bottom parts of cores from these sites.

70 Radioactive isotopes contained in the ice offer the opportunity to obtain absolute ages of  
71 an ice sample. For millennial scale ice cores,  $^{14}\text{C}$  dating is the technique of choice. With a  
72 half-life of 5370 years, dating in the age range from ~250 years to up to ten half-life times is  
73 theoretically possible, covering the time range accessible by alpine glaciers in the vast majority  
74 of cases (Uglietti et al., 2016). ~~The  $^{14}\text{C}$  dating of approach using~~ water insoluble organic carbon  
75 (WIOC) from glacier ice has become a well-established technique for ice core dating. ~~Samples~~  
76 ~~of >10  $\mu\text{g}$  WIOC can be dated with reasonable uncertainty (10-20%), requiring less than 1 kg~~  
77 ~~of ice from typical mid-latitude and low-latitude glaciers and its accuracy was recently~~  
78 ~~validated (Uglietti et al., 2016). Ice samples from mid- and low-latitude glaciers can now be~~  
79 ~~dated with a reasonable uncertainty of 10-20%. Ice sample masses of 200-800 g are usually~~  
80 ~~selected to aim for >10  $\mu\text{g}$  carbon for  $^{14}\text{C}$  analysis with accelerator mass spectrometry (AMS),~~  
81 ~~whereby the respective mass depends on sample age and organic carbon concentrations (Jenk~~  
82 ~~et al., 2007; Jenk et al., 2009; Sigl et al., 2009; Uglietti et al., 2016). However; Hoffmann et al.,~~  
83 ~~2018). Accordingly,~~ the low WIOC concentration in some glaciers and in Polar Regions, ~~with~~  
84 ~~and the corresponding related~~ large demands of ice mass puts a limit to this application.

85 Concentrations of dissolved organic carbon (DOC) in glacier ice are a factor of 2-8 higher  
86 compared to typical WIOC concentrations (Legrand et al., 2007; Legrand et al., 2013; May et  
87 al., 2013, Fang et al., in prep.). Using the DOC fraction for  $^{14}\text{C}$  dating could therefore reduce  
88 the required amount of ice or, for sample sizes similar to what would be needed for  $^{14}\text{C}$  dating  
89 by WIOC, improve the achievable analytical (dating) precision which strongly depends on the  
90 absolute carbon mass even for state-of-the-art micro-radiocarbon dating. The underlying  
91 hypothesis of applying the DOC fraction for  $^{14}\text{C}$  dating is the same as for the WIO $^{14}\text{C}$  dating  
92 approach (Jenk et al., 2006; Jenk et al., 2007; Jenk et al., 2009). DOC in ice is composed of  
93 atmospheric water soluble organic carbon (WSOC) contained in carbonaceous aerosol particles  
94 and organic gases taken up during precipitation (Legrand et al., 2013). WSOC is formed in the  
95 atmosphere by oxidation of gases emitted from the biosphere or from anthropogenic sources  
96 (Legrand et al., 2013; Fang et al. in prep.) -and subsequent condensation of the less volatile  
97 products. Carbonaceous aerosols transported in the atmosphere can be deposited on a glacier  
98 by wet and dry deposition. Before the industrial revolution, these organic carbon species, then  
99 entirely of non-fossil origin, contain the contemporary atmospheric  $^{14}\text{C}$  signal of the time when  
100 the snow deposited on the glacier (Jenk et al., 2006). ~~In view of the analytical precision~~  
101 ~~achievable with this method, the turn over time from atmospheric  $\text{CO}_2$  to deposited aerosol is~~  
102 ~~negligible (Fang et al., in prep.).~~ For both WIOC and WSOC, carbon from biomass burning  
103 and oceanic organic matter can potentially introduce a reservoir effect (sources of aged carbon).  
104 The mixed age of trees in Swiss forests today is estimated to be slightly less than 40 years  
105 (Mohn et al., 2008). Back in time, prior to extensive human forest management, the mixed age  
106 of trees in Europe was likely older and the mean age of old-growth forest wood ranged from  
107 around 70 to 300 years depending on the region, i.e. the tree species present (Gavin, 2001,  
108 Zhang et al., 2017). Prior to the use of fossil fuels about 50% of WIOC is estimated to originate  
109 from biomass burning (Minguillon et al., 2011). For biogenic DOC, May et al. (2013) estimated  
110 a turnover-time of around 3 to 5 years, corresponding to a 20% contribution from biomass  
111 burning. With a mean age of burned material (aged wood plus grass and bushes) of  $150\pm 100$   
112 years, this results in a potential in-built age from biomass burning for WIOC and DOC of  $75\pm 50$   
113 and  $30\pm 20$  years, respectively. Such an in-built age is negligible considering the analytical  
114 uncertainty, which is similarly the case for a bias from oceanic sources, since concentrations  
115 of marine organic tracers are more than one order of magnitude lower than terrestrial tracers  
116 for the vast majority of glacier sites. This conclusion is supported by the fact that Uglietti et al.  
117 (2016) did not identify such a bias, when comparing WIO $^{14}\text{C}$  ages with ages derived by  
118 independent methods.

119 For analyzing  $\text{DO}^{14}\text{C}$  in ice cores, one of the major limitations is the relatively low  
120 extraction efficiency ranging from 64% (Steier et al., 2013) to 96% (May et al., 2013; Fang  
121 et al., 2019) and the high risk of sample contamination (Legrand et al., 2013) potentially  
122 introduced during drilling, storage, and sample processing. A first attempt to use DOC for  $^{14}\text{C}$   
123 dating of ice samples was conducted by May (2009) using a set-up for a combined analysis of  
124 both, the DOC and WIOC fraction with subsequent radiocarbon micro-analysis. However,  
125 these first results suggested a potential in-situ production of  $^{14}\text{C}$  in the DOC fraction based on  
126 the obtained super modern  $F^{14}\text{C}$  values (i.e.  $F^{14}\text{C}$  values higher than ever observed in the recent  
127 or past ambient atmosphere). Building on these initial findings, May (2009) questioned the  
128 applicability of the DOC fraction for radiocarbon dating. Although the in-situ  $^{14}\text{C}$  production  
129 of  $^{14}\text{CO}$  and  $^{14}\text{CO}_2$  in air bubbles contained in polar ice has been studied thoroughly and is  
130 rather well understood (Van de Wal et al., 1994; Lal et al., 1997; Smith et al., 2000), possible  
131 mechanisms of  $^{14}\text{C}$  in-situ production followed by formation ~~in~~of organic compounds ~~seem far~~  
132 ~~less likely and have~~are not ~~been investigated and only few studies exist~~ to date (Woon, 2002);  
133 Hoffmann, 2016). To further explore the potential of  $\text{DO}^{14}\text{C}$  for dating ice, a DOC extraction  
134 setup for radiocarbon analyses was designed and built at the Paul Scherrer Institut (PSI). In  
135 order to minimize potential contamination, the entire system is protected from ambient air by  
136 inert gas (helium) flow or vacuum. To maximize the oxidation efficiency, the PSI DOC  
137 methodology applies an ultraviolet (UV) photochemical oxidation step supported by addition  
138 of Fenton's reagent. The setup has been characterized by a high extraction efficiency of 96%  
139 and a low overall process blank being superior in the resulting blank to sample ratio compared  
140 to other systems (Fang et al., 2019). The system can handle samples with volumes of up to  
141 ~350 mL ~~allowing  $^{14}\text{C}$  analysis on~~. With this volume, samples with DOC concentrations as  
142 low as 25-30  $\mu\text{g}/\text{kg}$  can be analyzed, yielding the minimal carbon mass required for reliable  
143  $^{14}\text{C}$  analysis (~10  $\mu\text{g}$  C). Pooling samples from several subsequent extractions would be  
144 feasible, allowing dating of samples with lower DOC concentration. In this study, we evaluate  
145  $^{14}\text{C}$  dating with the DOC fraction by comparing to results from the well- established and  
146 validated WIO $^{14}\text{C}$  dating method. This is not only analytically highly challenging, but also  
147 because of the very limited availability of the precious sampling material needed in a rather  
148 large quantity ~~(total for both fractions > 500 g) and~~, ideally covering a wide range of ages  
149 from a few hundred to several thousands of years. Here, we succeeded to analyze such parallel  
150 samples from four different Eurasian glaciers ~~were analyzed in parallel~~.

151

## 2 Sample preparation and <sup>14</sup>C analysis

To validate the DOC <sup>14</sup>C dating technique, a total of 17 ~~samples~~ice sections from the deep parts of ice cores from the four glaciers Colle Gnifetti, Belukha, Chongce (Core 1), and ~~Shule Nanshan~~Shu Le Nan Shan (SLNS) were selected (Figure 1). They were sampled in parallel to directly compare DOC and WIOC concentrations and <sup>14</sup>C dating results. The high-alpine glacier Colle Gnifetti is located in the Monte Rosa massif of the Swiss Alps, close to the Italian border. A 76 m long core was retrieved from the glacier saddle in September 2015 at an altitude of 4450 m asl. (45°55'45.7''N, 7°52'30.5''E); Sigl et al., 2018), only 16 m away from the location of a previously dated core obtained in 2003 (Jenk et al., 2009). The low annual net accumulation rate at this site (~0.45 m w.e. yr<sup>-1</sup>) provides access to old ice covering the Holocene (Jenk et al., 2009). Four samples were selected from the bottom 4 m (~~72-76 m~~) closest to bedrock (~~72-76 m depth~~). The Belukha core was drilled in May/June 2018 from the saddle between the two summits of Belukha (49°48'27.7''N, 86°34'46.5''E, 4055 m asl.), the highest mountain in the Altai mountain range. The bedrock was reached and the total length of the core is 160 m. Three samples were analyzed from the deepest part (158-160 m). Seven, and three samples were analyzed from the deep parts of SLNS and Chongce, respectively. The SLNS ice core was retrieved in May 2010 from the south slope of the ~~Shulenanshan~~Shu Le Nan Shan Mountain (38°42'19.35''N, 97°15'59.70''E, 5337 m asl.). The bedrock was reached and the total length of the ice core is 81.05 m (Hou et al., submitted). The Chongce ice cap is located in the western Kunlun Mountains on the northwestern Tibetan Plateau, covering an area of 163.06 km<sup>2</sup> with a volume of 38.16 km<sup>3</sup>; (Hou et al., 2018). The ice analyzed in this study was sampled from Chongce Core 1, one of three ice cores drilled in October 2012 (35°14'5.77''N, 81°7'15.34''E, 6010 m asl.). Two of those cores reached bedrock with lengths of 133.8 m (Core 1) and 135.8 m (Core 2). In 2013, two more ice cores were recovered ~~to~~from a higher altitude of 6100 m asl., reaching bedrock with lengths of 216.6 m (Core 4) and 208.6 m (Core 5) ~~at a higher altitude of 6100 m asl.~~ (Hou et al., 2018). ~~Find~~The annual net accumulation rate is about 0.14 m w.e. yr<sup>-1</sup> for Core 3, located less than 2 km away from Core 1. A summary of the metadata for the study sites and ice cores can be found in the supplement (Table S1) and details about ~~all samples~~sampling depths and sample sizes in Table 1. No results from any of the cores analyzed in this study have been published previously.

All ~~sample~~sampled ice sections were decontaminated in a cold room (-20°C) by cutting off the surface layer (~3 mm). ~~Each sample was~~ and each section split into two parallel



185 ~~sections~~ samples to perform both WIOC and DOC  $^{14}\text{C}$  analysis. Samples for WIO $^{14}\text{C}$ -dating  
186 were prepared following the protocol described in Uglietti et al. (2016) with a brief summary  
187 provided in the following. In order to remove potential contamination in the outer layer of the  
188 ice core, pre-cut samples from the inner part of the core were additionally rinsed with ultra-  
189 pure water (Sartorius, 18.2 M $\Omega$ ×cm, TOC < 5ppb), resulting in samples masses ranging from  
190 ~300 to 600 g (Table 1). To dissolve carbonate potentially present in the ice, melted samples  
191 were acidified with HCl to pH < 2, before being sonicated for 5 min. Subsequently, the  
192 contained particles were filtered onto pre-baked (heated at 800 °C for 5 h) quartz fiber filters  
193 (Pallflex Tissueqtz-2500QAT-UP). In a second carbonate removal step, the filters were  
194 acidified 3 times with a total amount of 50  $\mu\text{L}$  0.2M HCl, left for 1 h, rinsed with 5 mL ultra-  
195 pure water and finally left again for drying. These initial steps were performed in a laminar  
196 flow box to ensure clean conditions. At the Laboratory for the Analysis of Radiocarbon with  
197 AMS (LARA) of the University of Bern the particle samples were then combusted in a thermo-  
198 optical OC/EC analyzer (Model4L, Sunset Laboratory Inc, USA) equipped with a non-  
199 dispersive infrared (NDIR) cell to quantify the  $\text{CO}_2$  produced, using the well-established Swiss  
200 4S protocol for OC/EC separation (Zhang et al., 2012). Being coupled to a 200 kV compact  
201 accelerator mass spectrometer (AMS, MIni CARbon DAting System MICADAS) equipped  
202 with a gas ion source via a Gas Interface System (GIS, Ruff et al., 2007; Synal et al., 2007,  
203 Szidat et al., 2014), the LARA Sunset-GIS-AMS system (Agrios et al., 2015; Agrios et al.,  
204 2017) allowed for final, direct online  $^{14}\text{C}$  measurements of the  $\text{CO}_2$  produced from the WIOC  
205 fraction.

206 For DO $^{14}\text{C}$  analysis, sample preparation follows the procedure described in Fang et al.  
207 (2019). After transfer of pre-cut samples to the laboratory and before being melted, samples  
208 were further decontaminated in the pre-cleaned melting vessel of the extraction setup by rinsing  
209 with ultrapure water ~~before being melted~~, (sample mass loss of about 20-30 %), all performed  
210 under helium atmosphere. Simultaneously, a pre-cleaning step was applied to remove potential  
211 contamination in the system. For this, 50 mL ultra-pure water was injected into the reactor and  
212 acidified with 1 mL of 85%  $\text{H}_3\text{PO}_4$ . To enhance the oxidation efficiency, 2 mL of 100 ppm  
213  $\text{FeSO}_4$  and 1 mL of 50 mM  $\text{H}_2\text{O}_2$  (Fenton's reagent) was also injected into the base water  
214 before turning on the UV lights for ~20 min, thereby monitoring the process via the online  
215 NDIR  $\text{CO}_2$  analyzer. After the ice melted, the meltwater was filtrated under helium atmosphere,  
216 using a pre-baked in-line quartz fiber filter. The sample volume was determined by measuring  
217 the reactor fill level. The filtrate was acidified by mixing with the pre-treated base water. After

218 degassing of CO<sub>2</sub> from inorganic carbon was completed as monitored by the CO<sub>2</sub>- detector, 1  
219 mL of 50 mM H<sub>2</sub>O<sub>2</sub> was injected into the reactor right before the irradiation started. During  
220 UV oxidation, water vapor was removed by cryogenic trapping at -60 °C and produced CO<sub>2</sub>  
221 was trapped in liquid nitrogen. All steps were carried out under a constant flow of helium. The  
222 sample CO<sub>2</sub> was further cleaned from residual water vapor and quantified manometrically  
223 before being sealed into a glass vial for offline <sup>14</sup>C analyses. The CO<sub>2</sub> gas from DOC in the  
224 glass vial was directly injected into the MICADAS using a cracking system for glass vials  
225 under vacuum, allowing to then carry the CO<sub>2</sub> gas in a helium flow to the AMS ion source  
226 (Wacker et al., 2013). Procedural blanks were determined and continuously monitored by  
227 processing and analyzing frozen ultra-pure water (Sartorius, 18.2 MΩ cm, TOC < 5ppb) similar  
228 to natural ice samples. They were prepared every time when cutting ice and then  
229 processed/analyzed along with the samples at least twice a week. Procedural blanks are 1.3±0.6  
230 µg C with an F<sup>14</sup>C of 0.69±0.15 (n=76) and 1.9±1.6 µg C with an F<sup>14</sup>C value of 0.68±0.13  
231 (n=30) for WIOC and DOC, respectively.

232 All <sup>14</sup>C results are expressed as fraction modern (F<sup>14</sup>C), which is the <sup>14</sup>C/<sup>12</sup>C ratio of the  
233 sample divided by the same ratio of the modern standard referenced to the year 1950 (NIST,  
234 SRM 4990C, oxalic acid II), both being normalized to -25‰ in δ<sup>13</sup>C to account for isotopic  
235 fractionation. All AMS F<sup>14</sup>C values presented here are finally corrected for the system and  
236 method characteristic contributions as reported previously (e.g. Uglietti et al., 2016 and Fang  
237 et al., 2019). For WIOC analysis using the Sunset-GIS-AMS system this includes a correction  
238 for the system background, i.e. constant contamination (0.91±0.18 µgC with F<sup>14</sup>C of  
239 0.72±0.11). For the cracking system applied for DOC samples the constant contamination is  
240 0.06±0.18 µgC with F<sup>14</sup>C of 0.50 ±0.11). Further corrections applied account for the AMS  
241 cross contamination (0.2% of the previous sample), and ~~procedure blanks (1.26±0.59 µgC with~~  
242 ~~F<sup>14</sup>C of 0.69±0.15 for WIOC samples and 1.9±1.6 µgC with a F<sup>14</sup>C value of 0.68±0.13 for~~  
243 ~~DOC samples)procedural blanks (see above).~~ All uncertainties were propagated throughout  
244 data processing until final <sup>14</sup>C calibration. These corrections, have a larger effect on low carbon  
245 mass samples (higher noise-to-sample ratio), resulting in a larger dating uncertainty. Therefore,  
246 we only discuss samples with a carbon mass larger than 10 µg as recommended in Uglietti et  
247 al. (2016). Radiocarbon ages are calculated following the law of radioactive decay using 5570  
248 years as the half-life of radiocarbon, thus age equals -8033 \* ln (F<sup>14</sup>C) with -8033 years being  
249 Libby's mean lifetime of radiocarbon. Radiocarbon ages are given in years before present (BP)  
250 with the year of reference being 1950 (Stuiver and Polach, 1977). To obtain calibrated <sup>14</sup>C ages,

251 the online program OxCal v4.3.2 with the IntCal13 radiocarbon calibration curve was used  
252 (Reimer et al., 2013; Ramsey, 2017). Calibrated ages, also given in years before present, are  
253 indicated with (cal BP) and denote the  $1\sigma$  range unless stated otherwise.

254

## 255 **3 Results**

256

### 257 **3.1 DOC and WIOC concentrations**

258

259 DOC concentrations are generally higher compared to the corresponding WIOC concentrations  
260 (Figure 2). For all samples from the four glaciers, the DOC/WIOC concentration ratio ranges  
261 from 1.2 to 4.0 with an average of  $1.9 \pm 0.6$  (Table 2). This is at the lower end of previously  
262 reported average DOC/WIOC ratios of 2-8 (Legrand et al., 2007; Legrand et al., 2013, Fang et  
263 al., in prep.). This is likely explained by temporal variability because most samples in this study  
264 are several thousand years old, whereas the literature data only covers the last few centuries,  
265 including values from the industrial period in which additional anthropogenic sources exist (e.g.  
266 fossil DOC precursors). It is interesting to note that the average DOC/WIOC ratio at Belukha  
267 (2.5) is higher compared to the other sites (Colle Gnifetti, SLNS and Chongce is 1.8, 1.7 and  
268 1.6, respectively). Because the Belukha glacier is surround by extensive Siberian Forests, the  
269 higher ratio may be explained by particularly high emissions of biogenic volatile organic  
270 compounds. This is corroborated by the observation that DOC concentrations are highest at  
271 this site ( $241 \pm 82 \mu\text{g}/\text{kg}$ ) (Figure 2). Absolute concentrations of DOC and WIOC are slightly  
272 lower at Colle Gnifetti ( $112 \pm 12 \mu\text{g}/\text{kg}$  and  $63 \pm 13 \mu\text{g}/\text{kg}$ , respectively) compared to the other  
273 three glaciers (Table 1 and 2). Mean DOC and WIOC concentrations in the ice from the Tibetan  
274 Plateau are  $211 \pm 28 \mu\text{g}/\text{kg}$  and  $123 \pm 19 \mu\text{g}/\text{kg}$  for SLNS and  $156 \pm 40 \mu\text{g}/\text{kg}$  and  $99 \pm 37 \mu\text{g}/\text{kg}$   
275 for Chongce, respectively. These values are higher compared to the pre-industrial (PI) average  
276 values found in European Alpine glaciers, not only compared to the few samples from Colle  
277 Gnifetti of this study, but also to previously reported values from the Fiescherhorn glacier with  
278 PI-DOC of  $\sim 95 \mu\text{g}/\text{kg}$  (Fang et al., in prep.) and PI-WIOC of  $\sim 30 \mu\text{g}/\text{kg}$  (Jenk et al., 2006),  
279 respectively; and from Colle Gnifetti with PI-WIOC of  $\sim 30 \mu\text{g}/\text{kg}$  (Legrand et al., 2007; Jenk  
280 et al., 2006).

281

### 282 **3.2 Radiocarbon results**

283

284 For all four sites,  $F^{14}C$  of both fractions (WIOC and DOC) decreases with depth, indicating the  
285 expected increase in age (Figure 2, Table 1 and 2). For three of the sites (Colle Gnifetti, Belukha  
286 and SLNS), the corresponding DOC and WIOC fractions yielded comparable  $F^{14}C$  values: ~~with~~  
287 ~~no statistical evidence for a significant difference (Mann-Whitney U-test,  $U=79.5$ ,  $n=14$ ,~~  
288  ~~$p=0.41>0.05$ ).~~ They scatter along the 1:1 ratio line ~~and~~, are significantly correlated (Pearson  
289 correlation coefficient  $r=0.987986$ ,  $p < .01$ ,  $n=14$ ) and both intercept ( $0.021025 \pm 0.033034$ )  
290 and slope ( $1.036034 \pm 0.048050$ ) are not significantly different from 0 and 1, respectively  
291 (Figure 3a3). Nevertheless, ~~Figure 2 and Figure 3a suggest~~ a slight systematic offset towards  
292 lower  $F^{14}C$  values for WIOC compared to DOC; ~~seems evident if looking at least for higher~~  
293  ~~$F^{14}C$  values. Figures 2 and 3.~~ This is particularly obvious for the ~~samples from~~ Chongce  
294 ~~samples~~, characterized by ~~a~~ high mineral dust load ~~(see and from a site of very high elevation~~  
295 ~~with low net accumulation. For these samples, the  $F^{14}C$  DOC-WIOC offset is significant~~  
296 ~~(discussion in Sect. 4.2) and for which  $F^{14}C$  values of DOC and WIOC differ significantly.4.3).~~

297 For all sites, the calibrated  $^{14}C$  ages from both ~~fraction~~fractions show an increase in age  
298 with depth (Table 3). The ages range from  $\sim 0.2$  to  $20.3$  kyr cal BP for DOC and  $\sim 0.98$  to  $22.4$   
299 kyr cal BP for WIOC, respectively. In both fractions, the oldest age was derived for the sample  
300 from the deepest part of the Belukha ice core. Samples from Colle Gnifetti generally showed  
301 younger ages ( $< 2$  kyr cal BP). The two ice cores from the Tibetan Plateau (SLNS and Chongce)  
302 cover a similar age span from  $\sim 0.2 \pm 0.1$  to  $5.5 \pm 0.3$  kyr cal BP in the DOC fraction. WIO $^{14}C$   
303 ~~gave~~resulted in a similar ~~ages~~age range for the samples from SLNS ( $0.98 \pm 0.4$  to  $6.6 \pm 0.8$  kyr  
304 cal BP), but ~~was considerably older~~ for Chongce ~~they resulted much older~~ ( $3.1 \pm 0.7$  to  $11.0 \pm 1.7$   
305 kyr cal BP, ~~see~~ discussion in ~~Section~~Sect. 4.2 and 4.3).

306

## 307 4 Discussion

308

### 309 4.1 Radiocarbon dating with the DOC fraction

310 In Table 3, we present the first radiocarbon dating results of ice using the DOC fraction, ~~with~~  
311 ~~the exception of one dating point being part of the dataset to establish the very recent, first~~  
312 ~~complete chronology of the Mt. Hunter ice core, Alaska (same setup and methodology as~~  
313 ~~described here, Fang et al., submitted).~~ The DOC calibrated  $^{14}C$  age of ice increases with depth  
314 for all four sites, as expected for undisturbed glacier archives from the accumulation zone. ~~The~~  
315 ~~fact that none of the samples analyzed in this study ( $n=17$ ) resulted in super modern  $F^{14}C$~~

316 values ( $> 1$ ) and the obtained significant correlation between the  $F^{14}C$  of WIOC and DOC (Sect.  
317 3.2) and the resulting calibrated  $^{14}C$  ages (Pearson  $r = 0.988$ ,  $p < .01$ ,  $n = 14$ , Figure S1) represent  
318 strong evidence against the previously suggested  $^{14}C$  in situ production in the DOC fraction  
319 (May, 2009). For samples from three out of the four sites, our results (Sect. 3) indicate no  
320 significant difference in  $F^{14}C$  between DOC and WIOC, with the latter fraction being validated  
321 for allowing accurate dating of the surrounding ice (Uglietti et al., 2016). With the new  $DO^{14}C$   
322 dating method an average dating uncertainty of around  $\pm 200$  years was achieved for samples  
323 with an absolute carbon mass of 20-60  $\mu g$ , if the and ice is younger than  $\sim 6$  kyr (Table 2).  
324 This and 3). The analytical uncertainty mainly arises from the correction for the procedure  
325 blank introduced during sample treatment prior to AMS analysis (see Sect. 2 for details about  
326 other corrections), contributing with 20 to 70 % to the final overall dating uncertainty. The  
327 contribution thereby depends on carbon mass (larger for small samples) and sample age (the  
328 larger the bigger the difference between sample and blank  $F^{14}C$ ). See how How the overall  
329 analytical uncertainty of  $F^{14}C$  decreases with higher carbon mass is shown in Figure S2 (see  
330 Sect. 2 for details on blank corrections). S1. For DOC concentrations observed in this study,  
331 an initial ice mass of about 250 g was required, with about 20-30 % of the ice being removed  
332 during the decontamination processes inside the DOC set-up, yielding  $\sim 200$  g of ice available  
333 for final analysis. Our Expected based on previously reported DOC/WIOC concentration ratios  
334 (Sect. 3.1), the results here confirmed that with this new technique, the required ice mass can  
335 thus be reduced by more than a factor of two compared to the mass needed for  $^{14}C$  dating using  
336 the WIOC fraction (expected based on the previously reported DOC/WIOC concentration ratio,  
337 Sect. 3.1). Consequently, using the DOC instead of the WIOC fraction for  $^{14}C$  dating, a higher  
338 dating precision can be achieved for ice samples of similar mass. An additional benefit is that  
339 the DOC extraction procedure allows monitoring to ensure complete the removal of inorganic  
340 carbon (for completeness (see Sect. 2), i.e. interfering carbonate which is important to avoid a  
341 potential age bias (see Sect. 4.2), leading to an improved accuracy. 3).

#### 343 4.2 Potential contribution of carbonates to $^{14}C$ of WIOC in situ production to $DO^{14}C$

344

345 As described in Section 3.2, no significant difference between  $F^{14}C$  of DOC and WIOC was observed  
346 for the ice samples from Colle Gnifetti, Belukha and SLNS (Figure 3). However, the observed offset  
347 for the samples from Chongee glacier needs to be discussed. Previously published WIOC  $^{14}C$  ages  
348 from the upper parts of the Chongee Cores 2 and

349 Previous studies suggested that  $^{14}\text{C}$  of the DOC fraction may be influenced by in-situ  
350 production of  $^{14}\text{C}$  in the ice matrix (May 2009; Hoffman 2016). Induced by cosmic radiation,  
351 the production of  $^{14}\text{C}$  atoms within the ice matrix, i.e. by spallation of oxygen within the water  
352 molecule, is a well-known process (Lal et al., 1987; Van de Wal et al., 1994). Earlier studies  
353 indicated that in-situ produced  $^{14}\text{C}$  atoms mostly form  $\text{CO}$ ,  $\text{CO}_2$  and  $\text{CH}_4$  (Petrenko et al.,  
354 2013), but also can form methanol and formic acid (Yankwich et al., 1946, Woon, 2002). The  
355 mechanism of incorporation of in-situ produced  $^{14}\text{C}$  incorporation into organic molecules is  
356 not well understood (Woon, 2002; Hoffman, 2016). Hoffmann (2016) performed neutron  
357 irradiation experiments on Alpine glacier ice, showing that about 11-25 % of the initially  
358 produced  $^{14}\text{C}$  atoms entered into the DOC fraction. The resulting effect on  $F^{14}\text{C}$  of DOC  
359 consequently depends on (i) the number of  $^{14}\text{C}$  atoms produced in the ice ( $^{14}\text{C}$  in-situ  
360 production), (ii) the fraction of these atoms incorporated into DOC, and because  $F^{14}\text{C}$  is based  
361 on a  $^{14}\text{C}/^{12}\text{C}$  ratio, (iii) the DOC concentration in the ice (the higher the smaller the resulting  
362 shift in  $F^{14}\text{C}$ -DOC).

363 The natural neutron flux, relevant for the  $^{14}\text{C}$  production rate, strongly depends on  
364 altitude and latitude with a generally uniform energy distribution of the incoming neutrons  
365 (Gordon et al., 2004). The  $^{14}\text{C}$  in-situ production in natural ice further depends on the depth in  
366 the glacier and the snow accumulation rate of the site (Lal et al., 1987), determining the totally  
367 received neutron radiation. Following Lal et al. (1987), the number of in-situ produced  $^{14}\text{C}$   
368 atoms in each of our ice samples was estimated, assuming an average incorporation into DOC  
369 of  $18\pm 7\%$  (Hoffmann, 2016) (Table 4, equations and input parameters in the Supplementary  
370 Material). The average  $F^{14}\text{C}$ -DOC shift for all samples is  $0.044\pm 0.033$ . We find a good  
371 correlation between the measured  $F^{14}\text{C}$  DOC-WIOC offset and the  $^{14}\text{C}$  in-situ caused  $F^{14}\text{C}$ -  
372 DOC shift which explains about 50 % of the offset (Pearson  $r=0.82$ , Figure 4) and after  
373 correcting for it improves the overall agreement between  $F^{14}\text{C}$  of DOC and WIOC (Figure 5).  
374 The shift is largest for the Chongce samples ( $0.109\pm 0.048$ ) as a result of the high production  
375 rate at 6 km altitude in combination with the low annual net accumulation rate at this site ( $0.14$   
376 m w.e.  $\text{yr}^{-1}$ ). The calculated shift for samples from the SLNS core, from similar latitude but  
377 from a site lower in altitude (5 km) and experiencing higher net accumulation ( $0.21$  m w.e.  $\text{yr}^{-1}$ ),  
378 is significant lower with  $0.038\pm 0.016$ . The samples from Belukha and Colle Gnifetti are  
379 least affected ( $0.013\pm 0.006$  and  $0.033\pm 0.013$ , respectively).

380 We find that while the effect of in-situ  $^{14}\text{C}$  production causes only a negligible shift in  
381  $F^{14}\text{C}$ -DOC for most samples (masked by the analytical uncertainty), it can become significant



382 for ice samples from sites of exceptional high altitude and experiencing low annual net  
383 accumulation rates in addition, such as the Chongce ice cap (6010 m asl., 0.14 m w.e. yr<sup>-1</sup>;  
384 Figure 4). Note that for any site, the size of this effect gets reduced the higher the DOC  
385 concentration of the sample.

### 387 4.3 Potential contribution of carbonates to <sup>14</sup>C of WIOC

388

389 Under the basic assumption that the initially emitted fractions of DOC and WIOC are of similar  
390 age, an additional contribution from <sup>14</sup>C-depleted carbonate (low F<sup>14</sup>C) to the WIOC would  
391 cause an F<sup>14</sup>C offset between the two fractions. Previously published WIOC <sup>14</sup>C ages from  
392 the upper parts of the Chongce Core 2 and Core 4, less than 2 and ~6 km away from Core 1,  
393 did show large scatter with no clear increase in age with depth for samples younger than 2  
394 kakyrns. It was speculated that this was at least partly caused by the visible, exceptionally high  
395 loading of mineral dust on the WIOC filters (Hou et al., 2018). Such high mineral dust loading  
396 was also observed during filtration of the Chongce Core 1 samples analyzed in this  
397 study presented here. High mineral dust content in the ice can influence <sup>14</sup>C dating with WIOC  
398 in two ways, by affecting filtration through clogging of the filter and by potentially contributing  
399 with <sup>14</sup>C-depleted carbon from carbonate, as has been discussed in most previous studies. They  
400 all concluded, that although for dust levels typically observed in ice cores from high elevation  
401 glaciers, no significant bias is detectable for <sup>14</sup>C of WIOC, but it was of concern for the  
402 elemental carbon (EC) fraction combusted at higher temperatures during OC/EC separation.  
403 ~~This fraction EC~~ – as well as total carbon (TC), the sum of OC and EC) – is thus not  
404 recommended to be used for radiocarbon dating (Jenk et al., 2006; Jenk et al., 2007; Jenk et al.,  
405 2009; Sigl et al., 2009; Uglietti et al., 2016). In any case of similar age of, the DOC  
406 and carbonate removal efficiency during WIOC fraction, a contribution of <sup>14</sup>C-depleted  
407 carbonate (low F<sup>14</sup>C) to WIOC would result in an F<sup>14</sup>C offset between the two fractions and  
408 yield a slope value different from 1, since it most strongly affects high F<sup>14</sup>C values (i.e. younger  
409 samples). This can easily be understood by the concept of isotopic mass balance. Therefore, to  
410 test sample preparation was never quantified.

411 Here, the hypothesis that incomplete removal of carbonate resulted in may have caused  
412 the F<sup>14</sup>C DOC-WIOC offset observed in remaining after accounting for DO<sup>14</sup>C in-situ  
413 production (Sect. 4.2) was tested. Applying an isotopic mass balance based model to our dataset,

414 ~~wethe carbonate removal efficiency in WIO<sup>14</sup>C samples was estimated the carbonate removal~~  
415 ~~efficiency of our procedure by applying an isotopic mass balance model. We thereby used the~~  
416 ~~The Ca<sup>2+</sup> concentration in the ice samples was thereby used as a tracer for calcium carbonate~~  
417 ~~(see Supplement for details see supplement). The obtained).~~

418 ~~We find a carbonate removal procedure incomplete by around 2 % (i.e. an average~~  
419 ~~removal efficiency of ~96% would amount to a 98±2 %) to be sufficient for explaining the~~  
420 ~~remaining part of the observed F<sup>14</sup>C DOC-WIOC offset Figure 5). In terms of residual~~  
421 ~~carbonate carbon mass on the filter of ~4, this equals to < 2 µgC on average (Table 4). The~~  
422 ~~effect of this not entirely complete removal, can easily explain the F<sup>14</sup>C DOC WIOC offset~~  
423 ~~observed for the Chongce ice core samples. By accounting for the estimated carbonate~~  
424 ~~contribution, the offset for these samples S2). On the one hand, this is significantly reduced to~~  
425 ~~the level of scatter observed for the three other sites (Figure 3b; for an according Figure in~~  
426 ~~agreement with calibrated <sup>14</sup>C ages instead of F<sup>14</sup>C see S1). Based on these model results, we~~  
427 ~~are also confident to conclude that residual carbonate carbon is the most likely cause to explain~~  
428 ~~the slight systematic F<sup>14</sup>C DOC WIOC shift we observed for the other three sites. The old~~  
429 ~~samples from Belukha contain the highest Ca<sup>2+</sup> concentrations in this study. With their origin~~  
430 ~~in the Late Glacial or Glacial to Holocene transition period, these samples might not be~~  
431 ~~comparable to the other samples in terms of mineral dust sources and transport. Their Ca<sup>2+</sup> to~~  
432 ~~carbonate ratio or the abundance of the more soluble form of bicarbonate can thus be assumed~~  
433 ~~to be at least slightly different compared to the rest of the samples with the determined average~~  
434 ~~removal efficiency thus yielding a slight underestimation for the samples from Belukha~~  
435 ~~(estimated to rather be ~99%, see Supplement). In any case, our results confirm the findings of~~  
436 ~~previous studies, indicating that the potential carbonate related bias for <sup>14</sup>C dating using WIOC~~  
437 ~~is hardly detectable for ice samples with normal dust loading, typically being less than the~~  
438 ~~analytical uncertainty (around 10-20% of the determined age, see supplement Figure S3). For~~  
439 ~~example, Uglietti et al. (2016) did not detect such an effect when comparing dating results from~~  
440 ~~WIO<sup>14</sup>C with ages from independent methods. (effect masked by the analytical uncertainty,~~  
441 ~~see Figure S2). For example, Uglietti et al. (2016) did not detect such an effect when~~  
442 ~~successfully validating WIO<sup>14</sup>C dating results with ages from independent methods. On the~~  
443 ~~other hand, it demonstrates that a slightly below average removal efficiency for ice samples~~  
444 ~~containing visibly high loading of mineral dust can already cause a notable offset (93-97 % for~~  
445 ~~Chongce). The likely bigger particle size in such samples will affect their solubility, i.e.~~  
446 ~~increase the dissolution time required in the acid treatment step. In the current procedure, this~~



447 time is not adjusted accordingly (Sect. 2). Based on these results, we consider a small offset  
448 from incomplete carbonate removal to be a very likely reason contributing to the measured  
449 F<sup>14</sup>C DOC-WIOC, i.e. resulting dating offset (Figure 5). Instead of a correction, which does  
450 not seem feasible for this effect because of large uncertainties and likely substantial site-to-site  
451 (sample-to-sample) variations, we suggest future improvement in the analytical procedure of  
452 the carbonate removal step (e.g. a slight increase in acid concentration and an increase of the  
453 reaction time).

#### 455 **4.34 DO<sup>14</sup>C ages in the context of published chronologies**

456

457 In the following we will discuss our new DO<sup>14</sup>C results in the context of ages from previous  
458 studies ~~(Table 5, Figure 4).~~ For final calibration of <sup>14</sup>C ages, most of those earlier studies took  
459 advantage of the assumption of sequential deposition in the archive, ~~which seems very~~  
460 ~~reasonable considering the~~ i.e. a continuous, undisturbed and preserved sequential deposition  
461 of annual snow layers on ~~top of each other on~~ the glacier surface. Particularly in case of  
462 relatively large analytical uncertainties compared to the age difference of the samples, the  
463 sequential deposition model can moderately constrain the probability distribution of the  
464 calibrated age range in each sample of the dataset. For consistency we applied the same  
465 calibration approach here by using the in-built OxCal sequence model (Ramsey, 2008). ~~For all~~  
466 ~~DO<sup>14</sup>C data presented in this study, there is~~ While the underlying assumption may not generally  
467 be valid for all sites, and individually needs to be carefully assessed, we find no difference in  
468 the calibrated ages using the sequence model and the ages from the conventional calibration  
469 approach ~~(Table 3).~~ for all DO<sup>14</sup>C data presented in this study (Table 3). Note, that no  
470 correction for a potential in-situ <sup>14</sup>C bias was applied to the DO<sup>14</sup>C data used here (Section  
471 4.2).

472 We obtained the oldest age of ~21 kyr cal BP for the bedrock ice at Belukha, indicating  
473 this glacier to be oldest and of Pleistocene origin ~~(Figure 4).~~ This is older than the previously  
474 reported age of ~11 kyr cal BP, ~~which~~ (Table 5, Figure 6). The latter age was ~~retrieved~~ obtained  
475 for ~~the~~ an ice core from the nearby Belukha West Plateau glacier extracted in 2003 (B03) ~~and~~  
476 ~~not from the saddle as the 2018 core (B18) analyzed in this study~~ (Aizen et al., 2016; Uglietti  
477 et al., 2016). ~~However,~~ opposed to the 2018 core extracted from the saddle (B18) analyzed in  
478 this study. Also, the according sample from B03 was from a slightly shallower depth (0.6-0.3

479 m above bedrock-) than the sample analyzed from B18 in this study. The age range modeled  
480 for B03 atfor the same depth above bedrock as sampled in this study (0.5-0 m) is in better  
481 agreement with ~28 kyr cal BP withand a very large uncertainty of ~15 kyr (Uglietti et al.,  
482 2016). ThusOverall, our new age for the oldest ice at Belukha thus reasonably agrees well-with  
483 thisthe previous result, but yields a much better constrained age with a strongly reduced  
484 uncertainty of  $\pm 4$  kyr. The two glaciers from the Tibetan Plateau (SLNS and Chongce) show  
485 very similar bottom ages of ~5-6 kyr cal BP; (Figure 6), which is in agreement with the  
486 previously reported age range of Tibetan Plateau glaciers (Hou et al., 2018). The bottom age  
487 of Chongce Core 1 determined here based on DO<sup>14</sup>C ( $5.6 \pm 0.3$  kyr cal BP) is slightly younger  
488 than the previously reported bottom age in Core 2 based on WIO<sup>14</sup>C ( $6.3 \pm 0.3$  kyr cal BP, Hou  
489 et al., 2018), which is likely related to in agreement with the influence of residual carbonates  
490 on the latter (findings discussed in Section 4.2 and 4.3. Nevertheless, our new age is still in the  
491 range of the previously estimated bottom age (Table 5, Figure 6). The bottom most sample of  
492 the Colle Gnifetti 2015 (CG15) core could not be dated because the small amount of ice  
493 available yielded an insufficient carbon mass of  $<10$   $\mu\text{g}$  for <sup>14</sup>C analysis. Previous WIO<sup>14</sup>C  
494 dating of a core obtained at Colle Gnifetti in 2003 (CG03) also revealed ice of Pleistocene  
495 origin with the ice at bedrock being older than 15 kyr cal BP (Jenk et al., 2009). TheAs expected,  
496 the age obtained in this study from a shallower depth was much younger with 1.2 kyr cal BP;  
497 but. This is in excellent agreement with the age of CG03 atfor a similar depth (~74 m below  
498 surface). This is; Table 5, Figure 6). We consider this as a clear indication that the CG15 ice  
499 core drilling did not reach bedrock.

500 Overall, the dating with DO<sup>14</sup>C results in ages which are in good agreement with the  
501 age ranges reported in earlier studies. Even though a contribution from in-situ <sup>14</sup>C to DO<sup>14</sup>C  
502 was not considered in the comparison here, we find that the dating by the DOC fraction does  
503 not lead to significantly different results compared to dating by WIO<sup>14</sup>C or cause a different  
504 interpretation about the oldest ice still present for any of the sites.

505

## 506 **5 Conclusion**

507

508 In this study, we evaluated and successfully validated the DO<sup>14</sup>C dating technique by directly  
509 comparing with direct comparison of dating results fromwith the well-established WIO<sup>14</sup>C  
510 dating-method onusing parallel ice samples. Achieving this goal was not only analytically

511 demanding but also highly challenging ~~because of~~due to the very limited availability of the  
512 sampling material, requiring ice in rather large quantities and spanning a wide range of ages.  
513 The obtained  $\text{DO}^{14}\text{C}$  ages for four different Eurasian glaciers, ranging from  $0.2 \pm 0.2$  to  $20.3$   
514  $\pm 4.1$  kyrs cal BP, agreed well with the respective  $\text{WIOC}^{14}\text{C}$  ages ( $0.98 \pm 0.4$  to  $22.54 \pm 1.1$  kyrs  
515 cal BP) and with previously published chronologies from these ice core sites. This underlines  
516 the great potential for applying  $\text{DO}^{14}\text{C}$  analysis for ice core dating. ~~Effects of in-situ  $^{14}\text{C}$~~   
517 ~~production on  $\text{DO}^{14}\text{C}$  ages, as suspected in previous studies, were not observed. Our data~~  
518 ~~confirmed that pre-industrial DOC concentrations are higher by a factor of about two than~~  
519 ~~WIOC concentrations in high alpine ice cores. With the new  $\text{DO}^{14}\text{C}$  dating method~~With this  
520 new method, an average dating uncertainty of around  $\pm 200$  years was achieved for samples  
521 with an absolute carbon mass  $> 20 \mu\text{g}$  and ages up to  $\sim 6$  ka. ~~For DOC concentrations observed~~  
522 ~~in this study, an initial ice mass of about 250 g was required. The sample mass can thus be~~  
523 ~~reduced by more than a factor of two compared to the mass needed for  $^{14}\text{C}$  dating using the~~  
524 ~~WIOC fraction. Furthermore, the new  $\text{DO}^{14}\text{C}$  dating revealed a slight age bias of the WIOC~~  
525 ~~fraction towards older ages, which however was found to be significant only for ice containing~~  
526 ~~high concentrations of mineral dust and in particular if younger than  $\sim 1000$  years, in agreement~~  
527 ~~with findings of previous studies. In any case, for this age range, other independent dating~~  
528 ~~methods exist and the use of these in combination with radiocarbon ages in a glaciological flow~~  
529 ~~model to derive a final ice core age-depth relationship provides additional constraint, thus~~  
530 ~~reducing potential bias, for these younger ice sections (less weight given to the potentially~~  
531 ~~biased radiocarbon ages in this range). Nevertheless, future work for improving the carbonate~~  
532 ~~removal procedure is encouraged to further increase the accuracy of  $^{14}\text{C}$  dating with the WIOC~~  
533 ~~fraction of  $> 20 \mu\text{g}$  and ages up to  $\sim 6$  kyrs. For DOC concentrations observed in this study, an~~  
534 ~~initial ice mass of about 250 g was required. Our data confirmed previous results that~~  
535 ~~concentrations of pre-industrial DOC are higher by about a factor two compared to WIOC~~  
536 ~~concentrations in high alpine ice cores. This shows that the required ice mass to achieve similar~~  
537 ~~precision is reduced by at least a factor of two for  $^{14}\text{C}$  dating when using the DOC instead of~~  
538 ~~the WIOC fraction. Accordingly, an improvement in precision can be achieved for same sample~~  
539 ~~mass. Compared to WIOC, a downside of using the DOC fraction for  $^{14}\text{C}$  dating is a more~~  
540 ~~demanding and time consuming extraction procedure. In addition, because of its higher~~  
541 ~~solubility and a related higher mobility of DOC in case of meltwater formation, this fraction is~~  
542 ~~only applicable for dating ice which had been cold throughout its “lifetime”. Beneficial~~  
543 ~~compared to WIOC, there is no potential for a dating bias by carbonates of mineral dust for~~  
544  ~~$\text{DO}^{14}\text{C}$ . However, our results confirm previously suggested potential dating biases from in-situ~~

545 <sup>14</sup>C causing DO<sup>14</sup>C dates to shift towards younger ages. While we find the effect to be small  
546 (at the level of analytical uncertainty), it may become significant for DO<sup>14</sup>C dating of ice  
547 samples from sites of e.g. exceptional high altitude, experiencing low annual net accumulation  
548 rates in addition. For such sites, a reasonably accurate correction to account for the age bias  
549 seems feasible according to our results, although at the cost of an increase in the final dating  
550 uncertainty. Nevertheless, we think this new dating method has a great potential to open up  
551 new fields for radiocarbon dating of ice for example from remote regions, where concentrations  
552 of organic impurities in the ice are particularly low.

553 ~~In summary the main benefits of DO<sup>14</sup>C dating of glacier ice compared to WIO<sup>14</sup>C dating are~~  
554 ~~the reduced ice amount required, or higher precision for the same sample mass. The DOC~~  
555 ~~fraction is not affected from potential carbonate bias from mineral dust with the applied~~  
556 ~~methodology and thus ensures high dating accuracy. This new dating method opens up new~~  
557 ~~fields for radiocarbon dating of ice for example from remote or Polar Regions, where~~  
558 ~~concentrations of organic impurities in the ice are particularly low. Compared to the WIO<sup>14</sup>C~~  
559 ~~dating, a downside is the more demanding and time consuming DOC extraction procedure and~~  
560 ~~because of its higher solubility, the higher mobility of DOC in case of meltwater, thus only~~  
561 ~~being applicable for dating ice which had been cold throughout its “lifetime”.~~

## 563 **Acknowledgements**

564 We thank Johannes Schindler for his great work in designing and building the DOC extraction  
565 system and the two drilling teams on Colle Gnifetti and Belukha for collecting high quality ice  
566 cores. We acknowledge funding from the Swiss National Science Foundation (SNF) for the  
567 Sinergia project Paleo fires from high-alpine ice cores ([CRSII2\\_154450](#)), which allowed ice  
568 core drilling on Colle Gnifetti and Belukha, [for the project Radiocarbon dating of glacier ice](#)  
569 [\(200021\\_126515\)](#), and for the project Reconstruction of pre-industrial to industrial changes of  
570 organic aerosols from glacier ice cores (200021\_182765). We acknowledge the funding from  
571 the National Natural Science Foundation of China (91837102, 41830644) for the Tibetan ice  
572 core drilling. We dedicate this study to Alexander Zapf, who died tragically while climbing in  
573 the Swiss Alps, before he could fulfil his dream of ice dating with DO<sup>14</sup>C.

## 574 **Data availability**

575 The data is provided in the Tables.

576 **Author contributions**

577 LF and TS performed <sup>14</sup>C analysis. LF, TS, TMJ, and MS wrote the manuscript while all  
578 authors contributed to the discussion of the results. MS designed the study.

579 **Competing interests**

580 The authors declare that they have no conflict of interest.

581

## 582 **References**

- 583 Agrios, K., Salazar, G., Zhang, Y.-L., Uglietti, C., Battaglia, M., Luginbühl, M., Ciobanu, V. G., Vonwiller,  
584 M. and Szidat, S.: Online coupling of pure O<sub>2</sub> thermo-optical methods—<sup>14</sup>C AMS for source  
585 apportionment of carbonaceous aerosols, *Nucl. Instrum. Methods Phys. Res. B.*, 361, 288-293,  
586 <https://doi.org/10.1016/j.nimb.2015.06.008>, 2015.
- 587 Agrios, K., Salazar, G. and Szidat, S.: A Continuous-Flow Gas Interface of a Thermal/Optical Analyzer  
588 With <sup>14</sup>C AMS for Source Apportionment of Atmospheric Aerosols, *Radiocarbon*, 59, 921-932,  
589 <https://doi.org/10.1017/RDC.2016.88>, 2017.
- 590 Aizen, E. M., Aizen, V. B., Takeuchi, N., Mayewski, P. A., Grigholm, B., Joswiak, D. R., Nikitin, S. A.,  
591 Fujita, K., Nakawo, M. and Zapf, A.: Abrupt and moderate climate changes in the mid-latitudes of  
592 Asia during the Holocene, *J. Glaciol.*, 62, 411-439, <https://doi.org/10.1017/jog.2016.34>, 2016.
- 593 Bolzan, J. F.: Ice flow at the Dome C ice divide based on a deep temperature profile, *J. Geophys. Res.*  
594 *Atmos.*, 90, 8111-8124, <https://doi.org/10.1029/JD090iD05p08111>, 1985.
- 595 ChongYi, E., Sun, Y., Li, Y. and Ma, X., The atmospheric composition changes above the West Kunlun  
596 Mountain, Qinghai-Tibetan Plateau, International Conference on Civil, Transportation and  
597 Environment, Atlantis Press, 2016.
- 598 Fang, L., Schindler, J., Jenk, T., Uglietti, C., Szidat, S. and Schwikowski, M. J. R.: Extraction of Dissolved  
599 Organic Carbon from Glacier Ice for Radiocarbon Analysis, *Radiocarbon*, 61, 681-694,  
600 <https://doi.org/10.1017/RDC.2019.36>, 2019.
- 601 Fang L., Cao F., Jenk T. M., Vogel A. L., Zhang Y.L., Wacker L., Salazar G., Szidat S., Schwikowski M.:  
602 Enhancement of carbonaceous aerosol during the 20th century by anthropogenic activities: insights  
603 from an Alpine ice core, in preparation.
- 604 Gavin, D. G., Estimation of inbuilt age in radiocarbon ages of soil charcoal for fire history studies.  
605 *Radiocarbon* 43, 27-44, 2001.
- 606 Gordon, M. S., Goldhagen, P., Rodbell, K. P., Zabel, T. H., Tang, H. H. K., Clem, J. M., & Bailey, P.  
607 Measurement of the flux and energy spectrum of cosmic-ray induced neutrons on the ground. *IEEE*  
608 *Transactions on Nuclear Science*, 51(6), 3427-3434, 2004.
- 609 Hoffmann H. M. Micro radiocarbon dating of the particulate organic carbon fraction in Alpine glacier  
610 ice: method refinement, critical evaluation and dating applications, PhD dissertation, Ruperto-Carola  
611 University of Heidelberg, <http://archiv.ub.uniheidelberg.de/volltextserver/20712/>, 2016.
- 612 Hoffmann, H., Preunkert, S., Legrand, M., Leinfelder, D., Bohleber, P., Friedrich, R., & Wagenbach, D.,  
613 A New Sample Preparation System for Micro-<sup>14</sup>C Dating of Glacier Ice with a First Application to a  
614 High Alpine Ice Core from CG (Switzerland). *Radiocarbon*, 60(2), 517-533. doi:10.1017/RDC.2017.99,  
615 2018.
- 616 Hou, S., Jenk, T. M., Zhang, W., Wang, C., Wu, S., Wang, Y., Pang, H. and Schwikowski, M. J. T. C.: Age  
617 ranges of the Tibetan ice cores with emphasis on the Chongce ice cores, western Kunlun Mountains,  
618 *The Cryosphere*, 12, 2341-2348, <https://doi.org/10.5194/tc-12-2341-2018>, 2018.
- 619 Hou, S., Zhang W., Fang L., Jenk T.M., Wu S., Pang H., Schwikowski M., Brief Communication: New  
620 evidence further constraining Tibetan ice core chronologies to the Holocene, Submitted to *The*  
621 *Cryosphere*.  
622

623 Jenk, T. M., Szidat, S., Schwikowski, M., Gaggeler, H. W., Brutsch, S., Wacker, L., Synal, H. A. and  
624 Saurer, M.: Radiocarbon analysis in an Alpine ice core: record of anthropogenic and biogenic  
625 contributions to carbonaceous aerosols in the past (1650-1940), *Atmos. Chem. Phys.*, 6, 5381-5390,  
626 2006.

627 Jenk, T. M., Szidat, S., Schwikowski, M., Gäggeler, H., Wacker, L., Synal, H.-A. and Saurer, M.:  
628 Microgram level radiocarbon ( $^{14}\text{C}$ ) determination on carbonaceous particles in ice, *Nucl. Instrum.*  
629 *Methods Phys. Res. B.*, 259, 518-525, <https://doi.org/10.1016/j.nimb.2007.01.196>, 2007.

630 Jenk, T. M., Szidat, S., Boliuss, D., Sigl, M., Gaeggeler, H. W., Wacker, L., Ruff, M., Barbante, C.,  
631 Boutron, C. F. and Schwikowski, M.: A novel radiocarbon dating technique applied to an ice core  
632 from the Alps indicating late Pleistocene ages, *J Geophys. Res. Atmos.*, 114,  
633 <https://doi.org/10.1029/2009JD011860>, 2009.

634 Lal, D., K. Nishiizumi, and J. R. Arnold.: In situ cosmogenic  $^3\text{H}$ ,  $^{14}\text{C}$ , and  $^{10}\text{Be}$  for determining the net  
635 accumulation and ablation rates of ice sheets, *Journal of Geophysical Research: Solid Earth* 92.B6  
636 4947-4952, 1987.

637 Lal, Devendra: *Cosmogenic in situ radiocarbon on the earth, Radiocarbon After Four Decades*,  
638 Springer, New York, NY, 146-161, 1992.

639 Lal, D., Jull, A. T., Burr, G. and Donahue, D.: Measurements of in situ  $^{14}\text{C}$  concentrations in Greenland  
640 Ice Sheet Project 2 ice covering a 17 - kyr time span: Implications to ice flow dynamics, *J. Geophys.*  
641 *Res. Oceans*, 102, 26505-26510, <https://doi.org/10.1029/96JC02224>, 1997.

642 Legrand, M., Preunkert, S., Schock, M., Cerqueira, M., Kasper-Giebl, A., Afonso, J., Pio, C., Gelencsér,  
643 A. and Dombrowski-Etchevers, I.: Major 20th century changes of carbonaceous aerosol components  
644 (EC, WinOC, DOC, HULIS, carboxylic acids, and cellulose) derived from Alpine ice cores, *J. Geophys.*  
645 *Res. Atmos.*, 112, <https://doi.org/10.1029/2006JD008080>, 2007.

646 Legrand, M., Preunkert, S., Jourdain, B., Guilhermet, J., Fain, X., Alekhina, I. and Petit, J. R.: Water-  
647 soluble organic carbon in snow and ice deposited at Alpine, Greenland, and Antarctic sites: a critical  
648 review of available data and their atmospheric relevance, *Clim. Past Discuss.*, 9, 2357-2399,  
649 doi:10.5194/cpd-9-2357-2013, 2013.

650 Licciulli, C., Bohleber, P., Lier, J., Gagliardini, O., Hoelzle, M. and Eisen, O.: A full Stokes ice-flow  
651 model to assist the interpretation of millennial-scale ice cores at the high-Alpine drilling site Colle  
652 Gnifetti, Swiss/Italian Alps, *J. Glaciol.*, 66, 35-48, <https://doi.org/10.1017/jog.2019.82>, 2020.

653 May, B. L. Radiocarbon microanalysis on ice impurities for dating of Alpine glaciers, Ph.D. thesis,  
654 University of Heidelberg, Germany, 127pp., 2009.

655 May, B., Wagenbach, D., Hoffmann, H., Legrand, M., Preunkert, S. and Steier, P.: Constraints on the  
656 major sources of dissolved organic carbon in Alpine ice cores from radiocarbon analysis over the  
657 bomb - peak period, *J. Geophys. Res. Atmos.*, 118, 3319-3327, <https://doi.org/10.1002/jgrd.50200>,  
658 2013.

659 Masarik, J., and Reedy, R. C. : Terrestrial cosmogenic-nuclide production systematics calculated.  
660 *Earth and Planet. Sci. Lett.* 136, 381-395, 1995.

661 Minguillon MC, Perron N, Querol X, Szidat S, Fahrni SM, Alastuey A, et al. Fossil versus contemporary  
662 sources of fine elemental and organic carbonaceous particulate matter during the DAURE campaign  
663 in Northeast Spain, *Atmos. Chem. Phys.* 11, 12067-12084, 2011.



664 Mohn, J., Szidat, S., Fellner, J., Rechberger, H., Quartier, R., Buchmann, B., & Emmenegger, L.  
665 Determination of biogenic and fossil CO<sub>2</sub> emitted by waste incineration based on <sup>14</sup>C and mass  
666 balances. *Bioresource Technology* 99, 6471-6479, 2008.

667 Nye, J.: On the theory of the advance and retreat of glaciers, *Geophys. J. Int.*, 7, 431-456, 1963.

668 Petrenko, V. V., Severinghaus, J. P., Smith, A. M., Riedel, K., Baggenstos, D., Harth, C., Orsi, A., Hua,  
669 Q., Franz, P., Takeshita, Y., Brailsford, G., Weiss, R. F., Buizert, C., Dickson, A., Schaefer, H.: High-  
670 precision <sup>14</sup>C measurements demonstrate production of insitu cosmogenic <sup>14</sup>CH<sub>4</sub> and rapid loss of  
671 insitu cosmogenic <sup>14</sup>CO in shallow Greenland firn. *Earth and Planet. Sci. Lett.* 365,190–197,2013.

672 Ramsey, C. B.: Deposition models for chronological records, *Quat. Sci. Rev.*, 27, 42-60,  
673 <https://doi.org/10.1016/j.quascirev.2007.01.019>, 2008.

674 Ramsey, C. B.: Methods for summarizing radiocarbon datasets, *Radiocarbon*, 59, 1809-1833,  
675 <https://doi.org/10.1017/RDC.2017.108>, 2017.

676 Reimer, P. J., Bard, E., Bayliss, A., Beck, J. W., Blackwell, P. G., Ramsey, C. B., Buck, C. E., Cheng, H.,  
677 Edwards, R. L., Friedrich, M., Grootes, P., Guilderson, T., Hafliðason, H., Hajdas, I., Hatté, C., Heaton,  
678 T., Hoffmann, D. L., Hogg, A. G., Hughen, K. A., Felix Kaiser, K., Kromer, B., Manning, S. W., Niu, M.,  
679 Reimer, R. W., Richards, D. A., Scott, E. M., Southon, J. R., Staff, R. A., Turney, C. S. and van der Plicht,  
680 J.: IntCal13 and Marine13 radiocarbon age calibration curves 0–50,000 years cal BP, *Radiocarbon*, 55,  
681 1869-1887, [https://doi.org/10.2458/azu\\_js\\_rc.55.16947](https://doi.org/10.2458/azu_js_rc.55.16947), 2013.

682 Ruff, M., Wacker, L., Gäggeler, H., Suter, M., Synal, H.-A. and Szidat, S.: A gas ion source for  
683 radiocarbon measurements at 200 kV, *Radiocarbon* 49, 307-314,  
684 <https://doi.org/10.1017/S0033822200042235>, 2007.

685 Sigl, M., Jenk, T. M., Kellerhals, T., Szidat, S., Gäggeler, H. W., Wacker, L., Synal, H.-A., Boutron, C.,  
686 Barbante, C. and Gabrieli, J.: Towards radiocarbon dating of ice cores, *J. Glaciol.*, 55, 985-996,  
687 <https://doi.org/10.3189/002214309790794922>, 2009.

688 Sigl, M., Abram, N., Gabrieli, J., Jenk, T. M., Osmont, D., and Schwikowski, M., 19th century glacier  
689 retreat in the Alps preceded the emergence of industrial black carbon deposition on high-alpine  
690 glaciers, *The Cryosphere*,12,3311-3331, <https://doi.org/10.5194/tc-12-3311-2018>, 2018.

691 Smith, A., Levchenko, V., Etheridge, D., Lowe, D., Hua, Q., Trudinger, C., Zoppi, U. and Elcheikh, A.: In  
692 search of in-situ radiocarbon in Law Dome ice and firn, *Nucl. Instrum. Methods Phys. Res. B.*, 172,  
693 610-622, [https://doi.org/10.1016/S0168-583X\(00\)00280-9](https://doi.org/10.1016/S0168-583X(00)00280-9), 2000.

694 Steier, P., Fasching, C., Mair, K., Liebl, J., Battin, T., Priller, A. and Golser, R., A new UV oxidation  
695 setup for small radiocarbon samples in solution. *Radiocarbon*, 55, 373-382, DOI:  
696 10.2458/azu\_js\_rc.55.16368, 2013.

697 Stuiver, M. and Polach, H. A.: Discussion reporting of <sup>14</sup>C data, *Radiocarbon* 19, 355-363, 1977.

698 Synal, H.-A., Stocker, M. and Suter, M.: MICADAS: a new compact radiocarbon AMS system, *Nucl.*  
699 *Instrum. Methods Phys. Res. B.*, 259, 7-13, <https://doi.org/10.1016/j.nimb.2007.01.138>, 2007.

700 Szidat, S., Salazar, G. A., Vogel, E., Battaglia, M., Wacker, L., Synal, H.-A. and Türlér, A.: <sup>14</sup>C analysis  
701 and sample preparation at the new Bern Laboratory for the Analysis of Radiocarbon with AMS  
702 (LARA), *Radiocarbon*, 56, 561-566, [10.2458/56.17457](https://doi.org/10.2458/56.17457),2014.

703 Thompson, L. G., Tandong, Y., Davis, M. E., Mosley-Thompson, E., Mashiotta, T. A., Lin, P.-N.,  
704 Mikhalenko, V. N. and Zagorodnov, V. S. J. A. o. G.: Holocene climate variability archived in the



705 Puruogangri ice cap on the central Tibetan Plateau, *Ann. Glaciol.*, 43, 61-69,  
706 <https://doi.org/10.3189/172756406781812357>, 2006.

707 Uglietti, C., Zapf, A., Jenk, T. M., Sigl, M., Szidat, S., Salazar Quintero, G. A. and Schwikowski, M.:  
708 Radiocarbon dating of glacier ice: overview, optimisation, validation and potential, *The Cryosphere*  
709 10, 3091-3105, [10.5194/tc-10-3091-2016](https://doi.org/10.5194/tc-10-3091-2016), 2016.

710 Van de Wal, R., Van Roijen, J., Raynaud, D., Van der Borg, K., De Jong, A., Oerlemans, J., Lipenkov, V.  
711 and Huybrechts, P.: From  $^{14}\text{C}/^{12}\text{C}$  measurements towards radiocarbon dating of ice. *Tellus B Chem.*  
712 *Phys. Meteorol.*, 46, 91-102, <https://doi.org/10.3402/tellusb.v46i2.15755>, 1994.

713 Wacker, L., Fahrni, S. M., Hajdas, I., Molnar, M., Synal, H. A., Szidat, S. and Zhang, Y. L.: A versatile gas  
714 interface for routine radiocarbon analysis with a gas ion source, *Nucl. Instrum. Methods Phys. Res.*  
715 *B.*, 294, 315-319, <https://doi.org/10.1016/j.nimb.2012.02.009>, 2013.

716 Woon, D. E.: Modeling gas-grain chemistry with quantum chemical cluster calculations. I.  
717 Heterogeneous hydrogenation of CO and H<sub>2</sub>CO on icy grain mantles. *The Astrophys. J.*, 569, 541-548,  
718 2002.

719 Yankwich, P. E., Rollefson, G. K., and Norris, T. H. (1946). Chemical Forms Assumed by C<sup>14</sup> Produced  
720 by Neutron Irradiation of Nitrogenous Substances. *J. Chem. Phys.*, 14, 131-140,1946.

721 Zhang, Y. L., Perron, N., Ciobanu, V. G., Zotter, P., Minguillón, M. C., Wacker, L., Prévôt, A. S. H.,  
722 Baltensperger, U. and Szidat, S.: On the isolation of OC and EC and the optimal strategy of  
723 radiocarbon-based source apportionment of carbonaceous aerosols, *Atmos. Chem. Phys.*, 12, 10841-  
724 10856, <https://doi.org/10.5194/acp-12-10841-2012>, 2012.

725 Zhang, Y., Yao, X. Wang, Y. Liu, and S. Piao, Mapping spatial distribution of forest age in China, *Earth*  
726 *and Space Science*, 4, 108–116, doi:10.1002/2016EA000177, 2017.

727

**Table 1** WIOC samples analyzed from Colle Gnifetti, Belukha, SLNS and Chongce ice cores.

Core section	Depth (m)	Ice mass (kg)	WIOC ( $\mu\text{g}$ )	Concentration ( $\mu\text{g}/\text{kg}$ )	Bern AMS Nr.	F <sup>14</sup> C ( $\pm 1\sigma$ )	<sup>14</sup> C age (BP, $\pm 1\sigma$ )
CG110	72.1-72.7	0.570	35.2	61.9 $\pm$ 3.3	11770.1.1	0.875 $\pm$ 0.011	1073 $\pm$ 105
CG111	72.7-73.4	0.539	38.7	71.8 $\pm$ 3.8	11771.1.1	0.848 $\pm$ 0.011	1321 $\pm$ 101
CG112	73.4-73.9	0.536	23.7	44.1 $\pm$ 2.4	11772.1.1	0.852 $\pm$ 0.015	1284 $\pm$ 143
CG113	73.9-74.6	0.549	39.8	72.4 $\pm$ 3.8	11773.1.1	0.786 $\pm$ 0.011	1937 $\pm$ 109
Belukha412	158.3-159.0	0.443	37.8	85.2 $\pm$ 4.5	11766.1.1	0.367 $\pm$ 0.010	8055 $\pm$ 211
Belukha414	159.5-160.3	0.336	27.8	82.6 $\pm$ 4.4	11768.1.1	0.212 $\pm$ 0.014	12473 $\pm$ 535
Belukha415	160.3-160.9	0.319	39.3	123.3 $\pm$ 6.5	11769.1.1	0.100 $\pm$ 0.011	18462 $\pm$ 899
SLNS101	56.8-57.5	0.420	41.5	98.9 $\pm$ 2.1	12325.1.1	0.902 $\pm$ 0.047	825 $\pm$ 420
SLNS113	64.7-65.4	0.427	45.3	106.1 $\pm$ 2.5	12324.1.1	0.852 $\pm$ 0.046	1284 $\pm$ 438
SLNS122	68.9-69.7	0.424	58.5	138.0 $\pm$ 3.6	12323.1.1	0.807 $\pm$ 0.046	1727 $\pm$ 459
SLNS127	71.8-72.5	0.483	50.9	105.3 $\pm$ 2.5	12322.1.1	0.695 $\pm$ 0.046	2921 $\pm$ 532
SLNS136	76.7-77.5	0.374	50.6	135.2 $\pm$ 3.0	12321.1.1	0.521 $\pm$ 0.046	5235 $\pm$ 706
SLNS139	78.9-79.6	0.485	61.2	126.3 $\pm$ 3.6	12320.1.1	0.521 $\pm$ 0.045	5232 $\pm$ 703
SLNS141-142	80.3-81.0	0.413	61.7	149.5 $\pm$ 3.8	12319.1.1	0.489 $\pm$ 0.046	5754 $\pm$ 750
CC237	126.0-126.7	0.352	22.4	63.7 $\pm$ 1.8	12328.1.1	0.704 $\pm$ 0.049	2815 $\pm$ 555
CC244	130.2-130.8	0.311	29.8	95.9 $\pm$ 2.2	12327.1.1	0.639 $\pm$ 0.048	3602 $\pm$ 600
CC252	133.4-133.8	0.174	23.8	136.7 $\pm$ 4.3	12326.1.1	0.316 $\pm$ 0.049	9256 $\pm$ 1250

**Table 2** DOC samples analyzed for Colle Gnifetti, Belukha, SLNS and Chongce ice cores.

Core section	Depth (m)	Ice mass (kg)	DOC ( $\mu\text{g}$ )	Concentration ( $\mu\text{g}/\text{kg}$ )	Bern AMS Nr.	F <sup>14</sup> C ( $\pm 1\sigma$ )	<sup>14</sup> C age (BP, $\pm 1\sigma$ )	DOC/WIOC
CG110	72.1-72.7	0.171	18.9	110.0 $\pm$ 2.7	11575.1.1	0.943 $\pm$ 0.030	474 $\pm$ 259	1.8
CG111	72.7-73.4	0.207	25.5	122.9 $\pm$ 3.0	11576.1.1	0.901 $\pm$ 0.021	836 $\pm$ 190	1.7
CG112	73.4-73.9	0.248	23.6	95.0 $\pm$ 2.3	11577.1.1	0.889 $\pm$ 0.021	943 $\pm$ 192	2.2
CG113	73.9-74.6	0.246	29.5	119.4 $\pm$ 2.9	11578.1.1	0.849 $\pm$ 0.016	1312 $\pm$ 151	1.7
Belukha412	158.3-159.0	0.172	28.5	165.0 $\pm$ 4.0	11581.1.1	0.315 $\pm$ 0.024	9284 $\pm$ 624	1.9
Belukha414	159.5-160.3	0.128	41.9	327.4 $\pm$ 7.9	11584.1.1	0.239 $\pm$ 0.019	11505 $\pm$ 648	4.0
Belukha415	160.3-160.9	0.102	23.7	231.0 $\pm$ 5.6	11585.1.1	0.144 $\pm$ 0.041	15584 $\pm$ 2365	1.9
SLNS101	56.8-57.5	0.238	44.0	184.9 $\pm$ 4.5	12458.1.1	0.972 $\pm$ 0.016	227 $\pm$ 131	1.9
SLNS113	64.7-65.4	0.213	39.4	185.2 $\pm$ 4.5	12459.1.1	0.942 $\pm$ 0.016	484 $\pm$ 137	1.7
SLNS122	68.9-69.7	0.234	57.9	248.0 $\pm$ 6.0	12460.1.1	0.773 $\pm$ 0.010	2073 $\pm$ 101	1.8
SLNS127	71.8-72.5	0.252	57.8	229.7 $\pm$ 5.5	12461.1.1	0.730 $\pm$ 0.009	2527 $\pm$ 101	2.2
SLNS136	76.7-77.5	0.220	48.3	219.1 $\pm$ 5.3	12462.1.1	0.657 $\pm$ 0.009	3380 $\pm$ 112	1.6
SLNS139	78.9-79.6	0.208	48.1	230.8 $\pm$ 5.6	12463.1.1	0.580 $\pm$ 0.009	4381 $\pm$ 131	1.8
SLNS141-142	80.3-81.0	0.246	43.8	177.5 $\pm$ 4.3	12464.1.1	0.550 $\pm$ 0.010	4809 $\pm$ 151	1.2
CC237	126.0-126.7	0.208	28.5	136.6 $\pm$ 3.3	12454.1.1	0.980 $\pm$ 0.023	161 $\pm$ 185	2.1
CC244	130.2-130.8	0.167	21.7	129.8 $\pm$ 3.1	12455.1.1	0.800 $\pm$ 0.018	1789 $\pm$ 185	1.4
CC252	133.4-133.8	0.120	24.3	202.5 $\pm$ 4.9	12456.1.1	0.546 $\pm$ 0.016	4854 $\pm$ 239	1.5

**Table 3** Calibrated WIO<sup>14</sup>C and DO<sup>14</sup>C ages using OxCal v4.3.2 with the Intcal13 radiocarbon calibration curve. Ages are given as the OxCal provided  $\mu$ -age  $\pm 1\sigma$ , which is the calibrated mean age accounting for the age probability distribution. In addition, calibrated ages derived when applying the OxCal sequence deposition model for further constraint are shown.

Core section	WIOC Cal age (cal BP)	WIOC Cal age with sequence (cal BP)	DOC Cal age (cal BP)	DOC Cal age with sequence (cal BP)
CG110	<del>1024</del> <u>±110</u> 1004±119	<del>1003</del> <u>±99</u> 968±1049	464±235	403±196
CG111	<del>1238</del> <u>±96</u> 1224±103	<del>1198</del> <u>±81</u> 1174±86	810±169	749±123
CG112	<del>1209</del> <u>±130</u> 1190±142	<del>1310</del> <u>±98</u> 1292±103	901±176	947±139
CG113	<del>1898</del> <u>±130</u> 1889±138	<del>1890</del> <u>±123</u> 1869±143	1222±153	1248±144
Belukha412	<del>8957</del> <u>±265</u> 8960±266	<del>8953</del> <u>±247</u> 8954±268	10695±867	<del>10701</del> <u>±861</u> 10686±865
Belukha414	<del>14780</del> <u>±781</u> 14796±782	<del>14741</del> <u>±691</u> 14802±774	13646±893	<del>15063</del> <u>±737</u> 13670±880
Belukha415	<del>22485</del> <u>±1112</u> 22441±1107	<del>22343</del> <u>±949</u> 22497±1107	20264±4073	<del>20605</del> <u>±3936</u> 20393±4033
SLNS101	<del>851</del> <u>±395</u> 848±396	<del>707</del> <u>±317</u> 701±315	250±145	226±137
SLNS113	<del>1298</del> <u>±452</u> 1297±453	<del>1264</del> <u>±333</u> 1255±331	480±131	505±111
SLNS122	<del>1775</del> <u>±513</u> 1769±514	<del>1902</del> <u>±427</u> 1901±4301	2057±129	2056±129
SLNS127	<del>3178</del> <u>±677</u> 3175±679	<del>3223</del> <u>±625</u> 3221±629	2585±125	2585±125
SLNS136	<del>6033</del> <u>±829</u> 6030±824	<del>5424</del> <u>±617</u> 5426±620	3635±138	3636±137
SLNS139	<del>6032</del> <u>±811</u> 6026±820	<del>6171</del> <u>±617</u> 7±567	5014±191	5007±187
SLNS141-142	<del>6619</del> <u>±841</u> 6626±831	<del>7069</del> <u>±676</u> 7081±689	5519±188	5531±176
	<del>3057</del> <u>±704</u>	<del>2956</del> <u>±564</u>		233±153
	<del>4050</del> <u>±764</u>	<del>4214</del> <u>±699</u>		1738±212
CC237	<del>10998</del> <u>±1689</u> 3051±703	<del>10948</del> <u>±1656</u> 2886±617	237±151	5580±295
CC244	<del>4057</del> <u>±769</u>	<del>4210</del> <u>±713</u>	1737±211	
CC252	<del>11000</del> <u>±1697</u>	<del>11017</del> <u>±1716</u>	5580±294	

**Table 4** Estimated residual carbonate carbon on the analyzed WIOC filters.  $\text{Ca}^{2+}$  concentrations, used here as a tracer for carbonates, are average values for the sampled ice core sections (or site if data not available) of which the mass is also indicated.

Core section	$\text{Ca}^{2+}$ concentration (ppb)	ice sample mass (kg)	residual carbonate-C ( $\mu\text{gC}$ )
CG110	100	0.570	0.3
CG111	110	0.539	0.3
CG112	61	0.536	0.2
CG113	59	0.549	0.2
Belukha412	4191	0.443	10.2
Belukha414	7566	0.336	13.9
Belukha415	3737	0.319	6.5
SLNS101	1400*	0.420	3.2
SLNS113	same	0.427	3.3
SLNS122	same	0.424	3.3
SLNS127	same	0.483	3.7
SLNS136	same	0.374	2.9
SLNS139	same	0.485	3.7
SLNS141-142	same	0.413	3.2
CC237	2170 <sup>#</sup>	0.352	4.2
CC244	same	0.311	3.7
CC252	same	0.174	2.1

\*No  $\text{Ca}^{2+}$  concentrations are available for SLNS, instead the average  $\text{Ca}^{2+}$  concentration over the last 7000 years measured on the nearby Puruogangri ice cap on the central Tibetan Plateau are used here (Thompson et al., 2006).

<sup>#</sup>  $\text{Ca}^{2+}$  concentration over the period of 1903–1992 from another core drilled on the Chongee ice cap by a different group (Chong Yi et al., 2016).

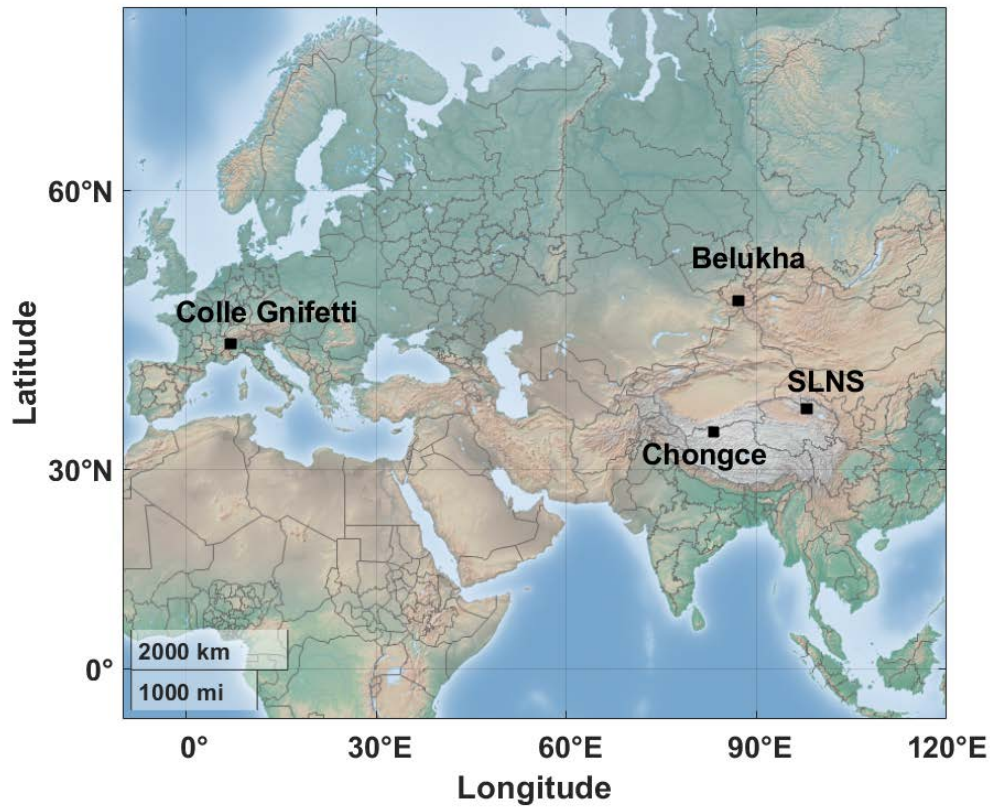
**Table 4** Estimate of the effect from in-situ  $^{14}\text{C}$  production on  $\text{F}^{14}\text{C}$ -DOC. For comparison, the measured  $\text{F}^{14}\text{C}$  offset between DOC and WIOC is also shown.

<u>Core section</u>	<u>Ice mass</u> (g)	<u>Carbon mass</u> ( $\mu\text{g}$ )	<u>Depth</u> (m w.e.)	<u><math>P_0</math></u> ( $^{14}\text{C}$ atom $\text{g}^{-1}$ ice $\text{yr}^{-1}$ )	<u>In-situ <math>^{14}\text{C}</math></u> (atoms)	<u>In-situ <math>\text{F}^{14}\text{C}</math>-DOC</u> offset	<u>Observed <math>\text{F}^{14}\text{C}</math></u> <u>DOC-WIOC</u> offset	<u>In-situ</u> <u>corrected <math>\text{F}^{14}\text{C}</math>-</u> <u>DOC</u>	<u>In-situ</u> <u>corrected DOC</u> <u>Cal age</u> <u>(cal BP)</u>
<u>CG110</u>	<u>171</u>	<u>18.9</u>	<u>55.8</u>	<u>328</u>	<u>1197</u>	<u>0.033±0.013</u>	<u>0.068±0.032</u>	<u>0.910±0.033</u>	<u>752±273</u>
<u>CG111</u>	<u>207</u>	<u>25.5</u>	<u>56.3</u>	<u>328</u>	<u>1197</u>	<u>0.030±0.012</u>	<u>0.053±0.024</u>	<u>0.901±0.024</u>	<u>1045±207</u>
<u>CG112</u>	<u>248</u>	<u>23.6</u>	<u>56.7</u>	<u>328</u>	<u>1197</u>	<u>0.038±0.015</u>	<u>0.037±0.026</u>	<u>0.889±0.026</u>	<u>1225±250</u>
<u>CG113</u>	<u>246</u>	<u>29.5</u>	<u>57.0</u>	<u>328</u>	<u>1197</u>	<u>0.030±0.012</u>	<u>0.064±0.019</u>	<u>0.849±0.020</u>	<u>1546±208</u>
<u>Belukha412</u>	<u>172</u>	<u>28.5</u>	<u>142.7</u>	<u>286</u>	<u>921</u>	<u>0.017±0.007</u>	<u>-0.052±0.026</u>	<u>0.315±0.025</u>	<u>11271±902</u>
<u>Belukha414</u>	<u>128</u>	<u>41.9</u>	<u>143.9</u>	<u>286</u>	<u>921</u>	<u>0.009±0.003</u>	<u>0.027±0.024</u>	<u>0.239±0.020</u>	<u>14096±964</u>
<u>Belukha415</u>	<u>102</u>	<u>23.7</u>	<u>144.5</u>	<u>286</u>	<u>921</u>	<u>0.012±0.005</u>	<u>0.043±0.043</u>	<u>0.144±0.041</u>	<u>21571±4753</u>
<u>\$LNS101</u>	<u>238</u>	<u>44</u>	<u>47.9</u>	<u>345</u>	<u>2666</u>	<u>0.044±0.017</u>	<u>0.070±0.050</u>	<u>0.972±0.023</u>	<u>587±187</u>
<u>\$LNS113</u>	<u>213</u>	<u>39.4</u>	<u>54.4</u>	<u>345</u>	<u>2656</u>	<u>0.044±0.017</u>	<u>0.089±0.050</u>	<u>0.942±0.023</u>	<u>837±184</u>
<u>\$LNS122</u>	<u>234</u>	<u>57.9</u>	<u>58.1</u>	<u>345</u>	<u>2651</u>	<u>0.033±0.013</u>	<u>-0.034±0.047</u>	<u>0.773±0.016</u>	<u>2483±210</u>
<u>\$LNS127</u>	<u>183</u>	<u>57.8</u>	<u>60.5</u>	<u>345</u>	<u>2647</u>	<u>0.026±0.010</u>	<u>0.029±0.047</u>	<u>0.730±0.014</u>	<u>2967±197</u>
<u>\$LNS136</u>	<u>220</u>	<u>48.3</u>	<u>64.7</u>	<u>345</u>	<u>2641</u>	<u>0.037±0.014</u>	<u>0.135±0.047</u>	<u>0.657±0.017</u>	<u>4264±304</u>
<u>\$LNS139</u>	<u>208</u>	<u>48.1</u>	<u>66.5</u>	<u>345</u>	<u>2638</u>	<u>0.035±0.014</u>	<u>0.058±0.046</u>	<u>0.580±0.016</u>	<u>5600±290</u>
<u>\$LNS141-142</u>	<u>246</u>	<u>43.8</u>	<u>67.7</u>	<u>345</u>	<u>2636</u>	<u>0.045±0.018</u>	<u>0.061±0.047</u>	<u>0.550±0.020</u>	<u>6323±363</u>
<u>CC237</u>	<u>208</u>	<u>28.5</u>	<u>113.7</u>	<u>497</u>	<u>5371</u>	<u>0.120±0.046</u>	<u>0.275±0.054</u>	<u>0.980±0.052</u>	<u>1240±498</u>
<u>CC244</u>	<u>167</u>	<u>21.7</u>	<u>117.6</u>	<u>497</u>	<u>5353</u>	<u>0.126±0.049</u>	<u>0.161±0.051</u>	<u>0.800±0.052</u>	<u>3509±799</u>
<u>CC252</u>	<u>120</u>	<u>24.3</u>	<u>120.2</u>	<u>497</u>	<u>5341</u>	<u>0.080±0.031</u>	<u>0.231±0.051</u>	<u>0.546±0.035</u>	<u>7007±635</u>

**Table 5** DO<sup>14</sup>C dating results for near bedrock ice compared to results from previous studies (visualized in Figure 46).

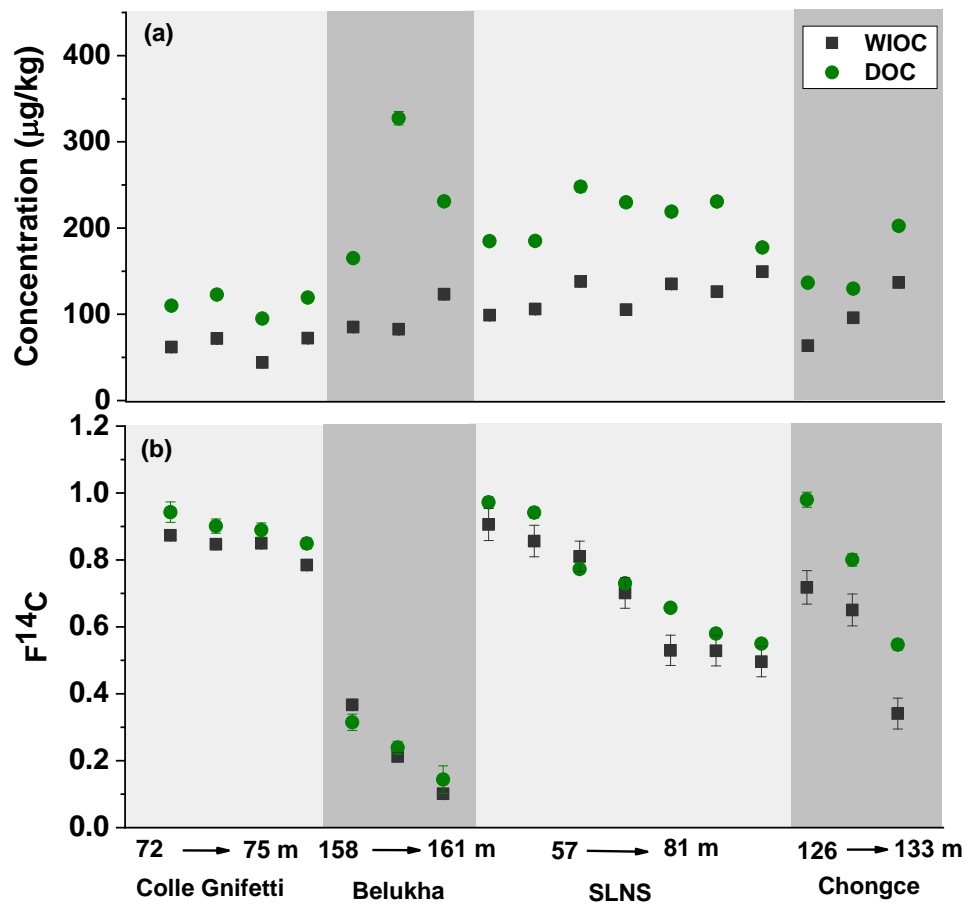
Site	Study	Core	Dating method	Depth above bedrock (m)	Age (cal BP)
Colle Gnifetti	this study	CG15	DO <sup>14</sup> C	(74.3 m below surface)*	1248 ± 144
	Jenk et al., 2009	CG03	WIO <sup>14</sup> C	(73.5 m below surface)#	1152 ± 235
	Jenk et al., 2009	CG03	Model	(74.3 m below surface)&	1160 ± <sub>170</sub> <sup>140</sup>
	Jenk et al., 2009	CG03	WIO <sup>14</sup> C	0.6-0	>15000
	Jenk et al., 2009	CG03	Model	oldest ice estimate	19100 ± <sub>4500</sub> <sup>4800</sup>
Belukha	this study	B18 (saddle)	DO <sup>14</sup> C	0.5-0	<del>20605 ± 3936</del> <u>20393 ± 4033</u>
	Aizen et al., 2016	B03 (west plateau)	WIO <sup>14</sup> C	0.6-0.3	11015 ± 1221
	Uglietti et al., 2016	B03 (west plateau)	Model	0.6-0	28500 ± 16200
SLNS	this study	SLNS	DO <sup>14</sup> C	0.4-0	5531 ± 176
	no previous results		---	---	---
Chongce	this study	Core 1	DO <sup>14</sup> C	0.2-0	5580 ± 295
	Hou et al., 2018	Core 2	WIO <sup>14</sup> C	1.2-0.8	6253 ± 277
	Hou et al., 2018	Core 2	Model	oldest ice estimate	9000 ± <sub>3600</sub> <sup>7900</sup>

\*precise bedrock depth unknown at this coring site, #sampled depth being closest to depth sampled in this study; (CG03 and CG15 drill sites only 16 m apart), & modeled age at same depth as sampled in this study.

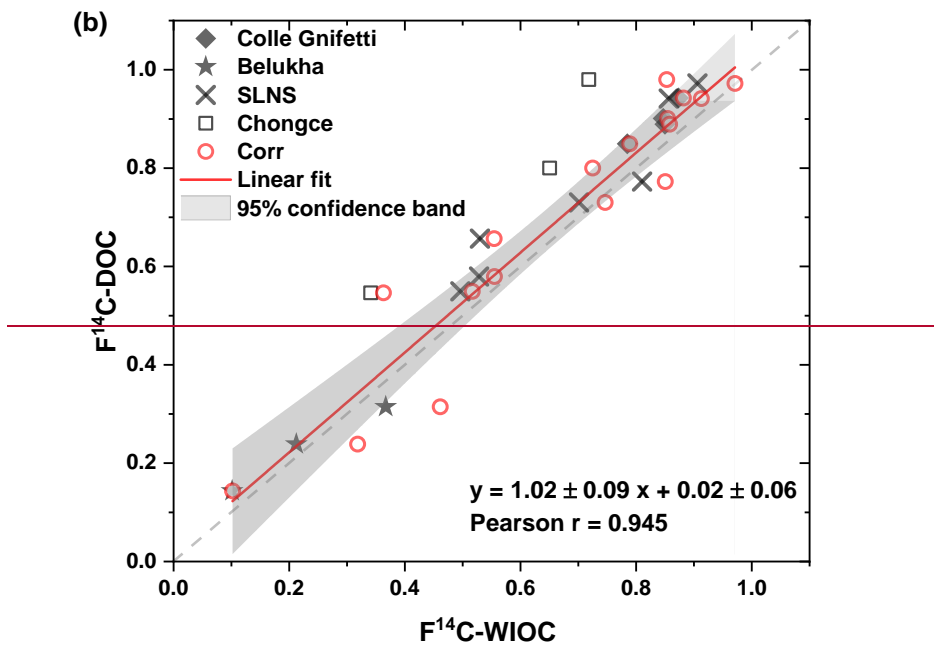
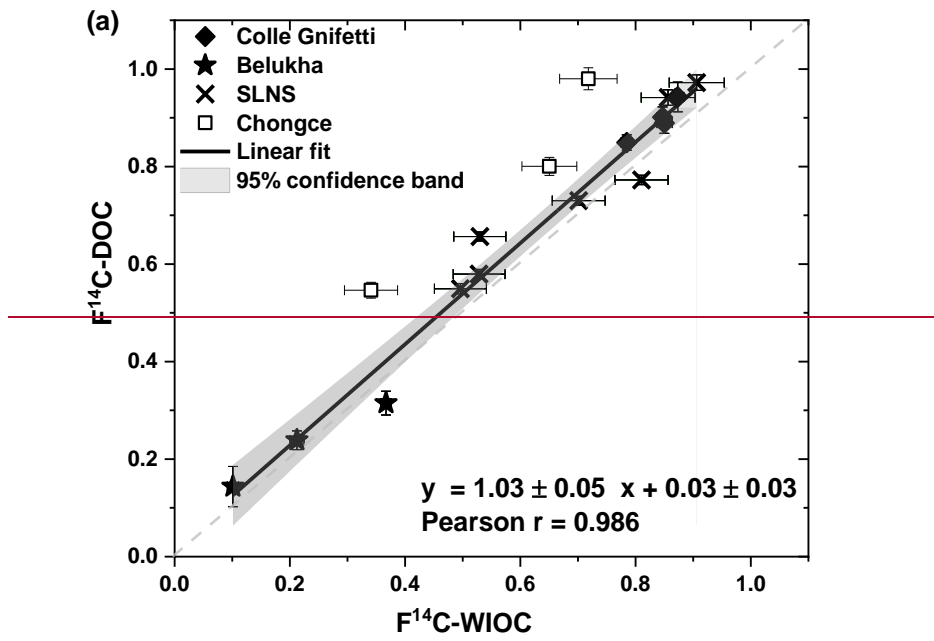


**Figure 1:** Location of the four glaciers Colle Gnifetti, Belukha, Chongce, and Shu Le Nan Shan (SLNS). Map made from Matlab R2019b geobasemap. Colle Gnifetti is located in the Monte Rosa massif in the Swiss Alps, Belukha glacier in the Altai mountain range, Russia, the Chongce ice cap on the northwestern Tibetan Plateau, China, and the SLNS at the south slope of the Shulenanshan Mountain, China.





**Figure 2:** Comparison of results from the WIOC and DOC fractions for the studied four sites. (a) concentrations (b)  $F^{14}\text{C}$ . The error bars denote the overall analytical  $1\sigma$  uncertainty.



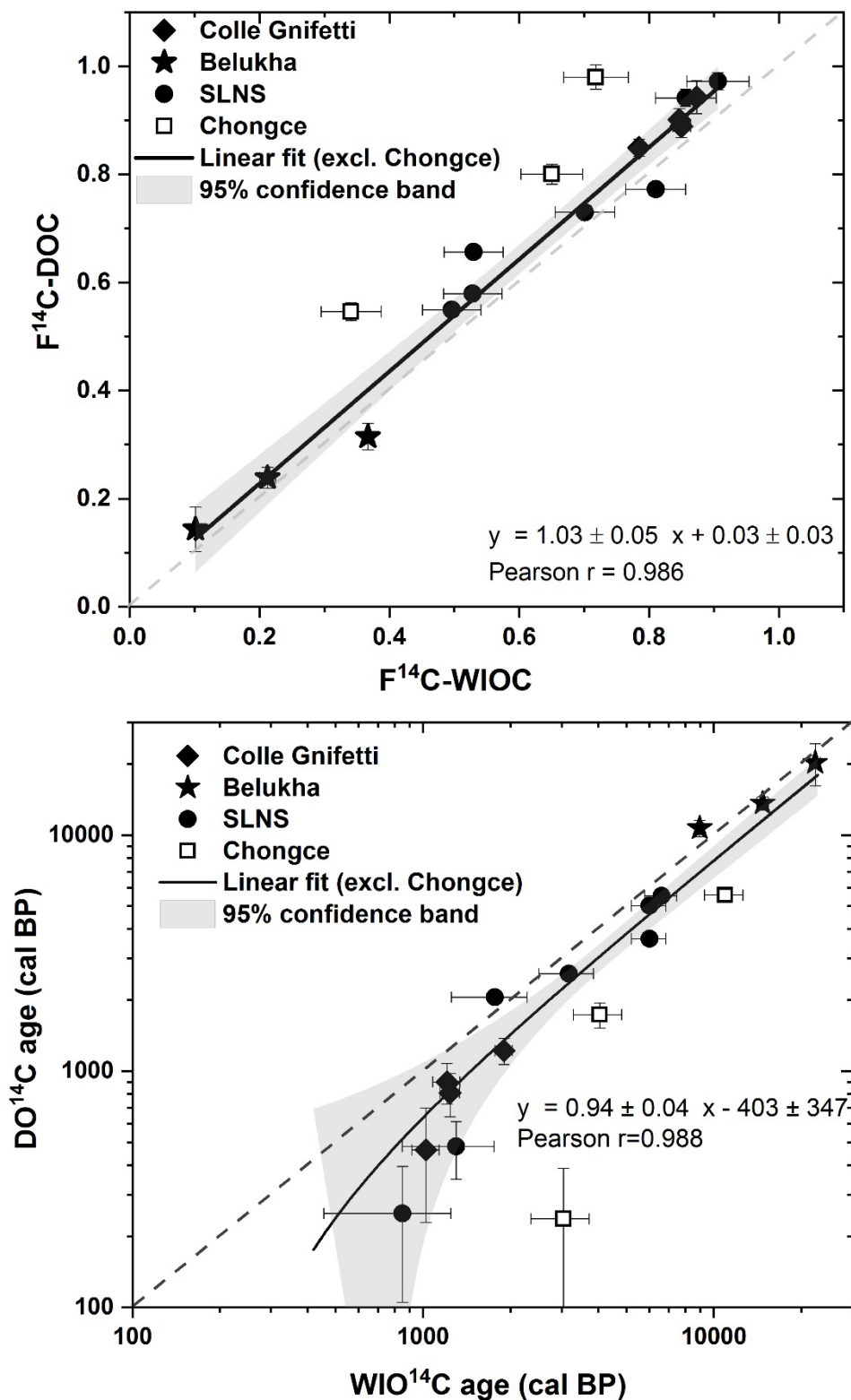


**Figure 3:** Scatter plot showing the correlation between  $F^{14}C$  of WIOC and DOC. (a) Measured values  $DO^{14}C$  results for the four sites (see legend). In terms of  $F^{14}C$  (top) and calibrated ages (bottom). For the linear fit shown in both panels, the data from Chongce (open symbols) was not excluded. Shaded areas indicate the 95% confidence band.

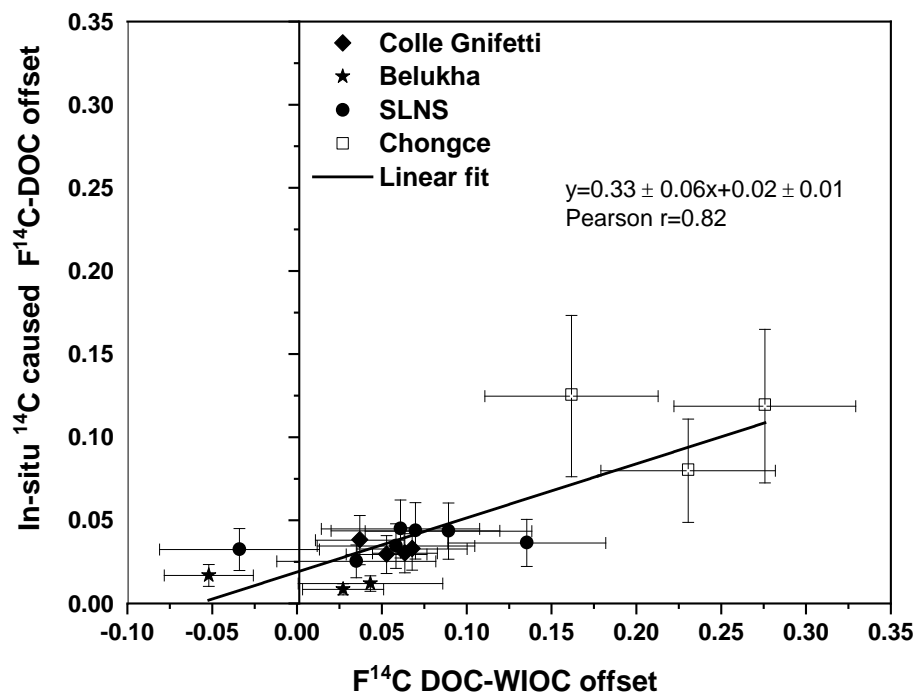


**Figure 4** Estimated in-situ  $^{14}\text{C}$  offset to  $\text{F}^{14}\text{C}$ -DOC plotted against the measured offset between  $\text{F}^{14}\text{C}$  of the DOC and WIOC fraction.

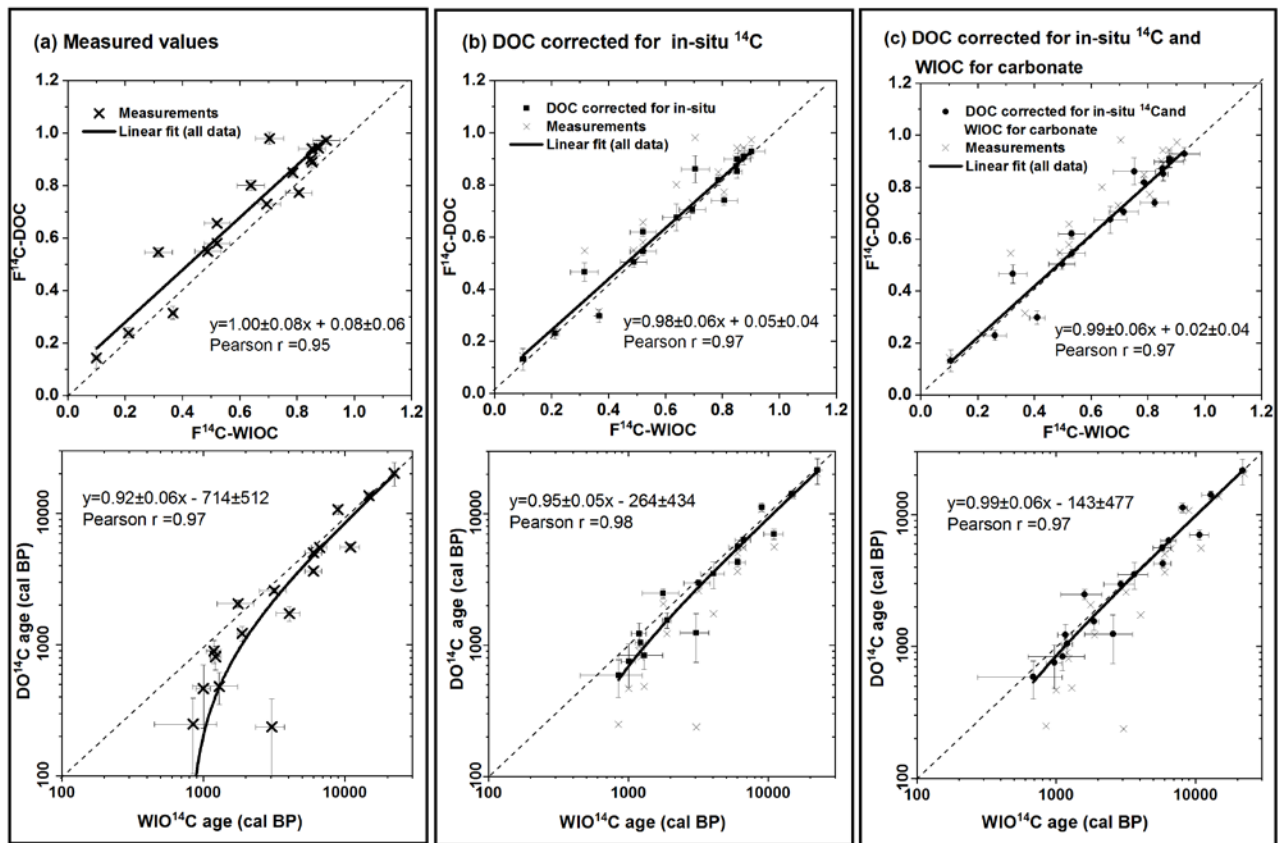


**Figure 5** Scatter plots showing the correlation between  $WIO^{14}C$  and  $DO^{14}C$  results for all samples. In terms of  $F^{14}C$  (top) and calibrated ages (bottom). (a) Measured values as shown in Figure 3 but with the linear fit applied to all data (Chongce included). (b) Same as panel (a), but  $DOC^{14}C$  results corrected for in-situ  $^{14}C$  contribution. (c) Same as panel (a), but  $DOC$  and  $WIOC^{14}C$  results corrected for in-situ  $^{14}C$  and accounting for potentially incompletely removed carbonate, respectively. An estimated average carbonate removal efficiency of  $98 \pm 2\%$  was used here. Error bars in panel (a) and (b) reflect the propagated uncertainty of analysis and correction. In panel (b) and (c), measured values are shown as gray crosses.

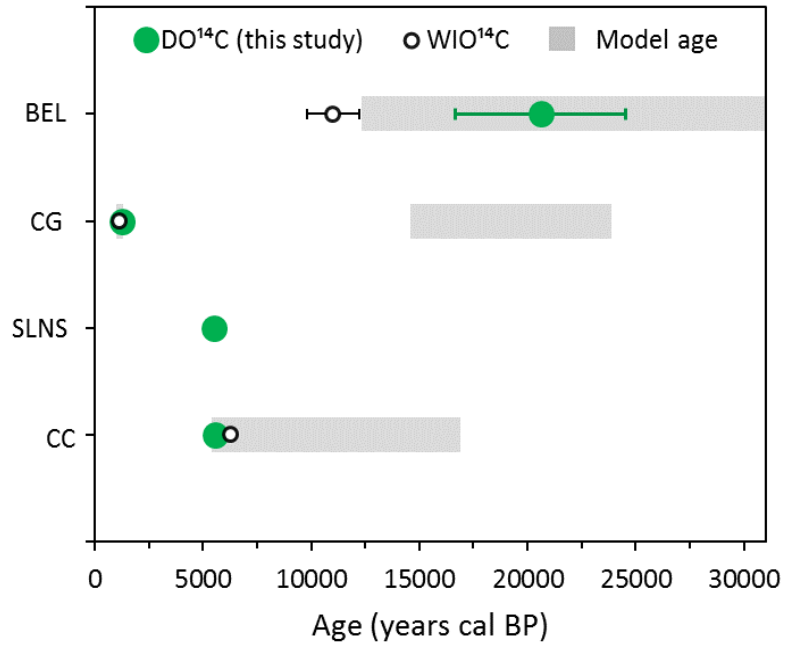


**Figure 4** Age of ice at the very bottom of the four glaciers (close to bedrock). DO<sup>14</sup>C dates, are shown

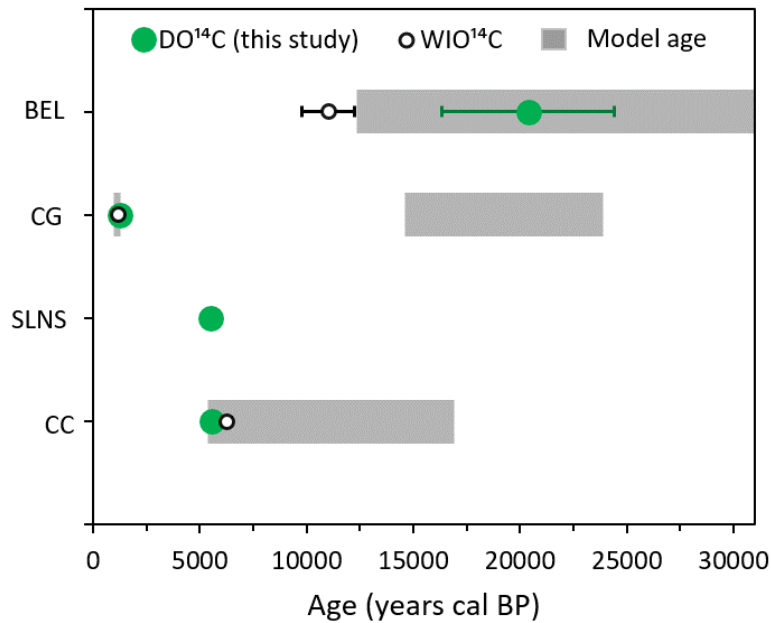


**Figure 6** Comparison of our DO<sup>14</sup>C ages (not corrected for in-situ) with dating results from previous studies if available. For the four sites of Belukha (BEL), Colle Gnifetti (CG), Shu Le Nan Shan (SLNS) and Chongce (CC), DO<sup>14</sup>C ages (green) and previously reported WIO<sup>14</sup>C ages indicated by open circles. The (open circles) for similar sampling depths are shown. Gray bars indicate previously modeled, <sup>14</sup>C based bedrock age estimates (additionally for CG the modeled estimate of age for the Belukha bottom age (gray bar) is sampling depth of this study). Previously published data are from Uglietti et al. (2016). The modeled Colle Gnifetti bottom age from (BEL, West Plateau), Jenk et al. (2009) and the indicated WIO<sup>14</sup>C value is from ice sampled from the CG03 core at similar depth as in this study. For Chongce, the result of the deepest WIOC sample from core 2 is shown together with the modelled bottom age ((CG), and Hou et al., (2018). Find all) (CC). See Table 5 for underlying data and information summarized in Table 5. details.

|